Landslide susceptibility assessment in the rocky coast subsystem of Essaouira – Morocco

Abdellah Khouz[1,2,3,4], Jorge Trindade[2,3,4], Sérgio C. Oliveira[3,4], Fatima El Bchari[5], Blaid Bougadir[1], Ricardo Garcia[3,4], Mourad Jadoud[6]

[1]Higher School of Technology Essaouira, Laboratory of Applied Sciences for the Environment and Sustainable Development (SAEDD), Cadi Ayyad University, Marrakech, Morocco.
[2]Universidade Aberta, Lisbon, Portugal.
[3]Centre of Geographical Studies, Institute of Geography and Spatial Planning, Portugal
[4]Associated Laboratory Terra, Portugal
[5]Polydisciplinary Faculty of Safi, Safi, Morocco, Department of Earth Sciences, Cadi Ayyad University, Marrakech.
[6]Faculty of sciences El Jadida, Geosciences and Environmental Techniques Laboratory, Chouaïb Doukkali University, El Jadida, Morocco.

Correspondence to: **A. Khouz** (abdellah.khouz@gmail.com)

Abstract

In recent decades, multiple researchers have produced landslide susceptibility maps using different techniques and models, including the information value method, which is a statistical model that is widely applied to various coastal environments. This study aimed to evaluate the susceptibility to landslides in the Essaouira coastal area using bivariate statistical methods. In this study, 588 distinct landslides were identified, inventoried, and mapped. They primarily result from the observation and interpretation of different data sources, namely, high-resolution satellite images, aerial photographs, topographic maps, and extensive field surveys. The rocky coastal system of Essaouira is located in the middle of the Atlantic coast of Morocco. The study area was split into 1534 cliff terrain units 50 m in width. For training and validation purposes, the landslide inventory was divided into two independent groups: 70% for training and 30% for validation. Twenty-two layers of landslide-conditioning factors were prepared, namely elevation, slope angle, slope aspect, plan curvature, profile curvature, cliff height, topographic wetness index, topographic position index, slope over area ratio, solar radiation, presence of faulting, lithological units, toe lithology, presence and type of cliff toe protection, layer tilt, rainfall, streams, land-use patterns, normalized difference vegetation index, lithological material grain size, and presence of springs. The statistical relationship between the conditioning factors and different landslide types was calculated using the bivariate information value method in a pixel and in the elementary terrain units-based model. Coastal landside susceptibility maps were validated using landslide training group partitions. The receiver operating characteristic curve and area under the curve were used to assess the accuracy and prediction capacity of the different coastal landslide susceptibility models. Two methodologies, considering a pixel-based approach and using coastal terrain units, were adopted to evaluate coastal landslide susceptibility. The results allowed for the classification of 38% of the rocky coast subsystem with high susceptibility to landslides, which were mostly located in the southern part of the Essaouira coastal area. These susceptibility maps will be useful for future planned development activities as well as for environmental protection.

Keywords: Coastal landslide susceptibility mapping, coastal landslide inventory, conditioning factors, Information Value, Essaouira coastal area, Morocco

1. Introduction

Landslides are common processes in the rocky coastal system of Essaouira. They result from the interaction of sub-aerial, marine, and anthropogenic processes (Trenhaile 1987; Sunamura 1992; Hampton and Griggs 2004; Greenwood and Orford; 2007), making this system more susceptible than any other natural system to anthropogenic pressure and erosional processes. Consequently, fast dynamic evolution imposes restrictions on the way humans occupy coastal areas (Teixeira 2006; Marques 2009; Teixeira 2015; Moore and Davis 2015; Gilham *et al.,* 2018).

The process of creating landslide susceptibility maps generally involves several qualitative or quantitative approaches, starting with landslide inventory as the first step for assessing landslide susceptibility, hazard, and risk (Aleotti and Chowdury 1999; Dai and Lee 2002; Van Westen *et al.,* 2008; Corominas *et al.,* 2014; Oliveira *et al.,* 2017; Meena *et al.,* 2018). For rocky coastal areas, landslide susceptibility/hazard assessments mainly address the evaluation of cliff retreat (Oliveira *et al.,* 2008; Rocha *et al.*, 2007; Oliveira *et al.,* 2017), landslide inventorying, and susceptibility mapping (Marques *et al., 2011*). The identification of factors controlling the rocky coast system is a critical step for better understanding how this system is evolving and to predict its future evolution (Neves and Ramos Pereira 1999). Landslides are responsible for significant erosion in rocky coastal systems (Andriani and Walsh 2007; Violante 2009; Sunamura 2015). Therefore, by knowing the set of predisposing factors that condition landslide occurrence, it is possible to spatially predict where future landslides will occur (Varnes 1984). Many different landslide-conditioning factors play an important role in the preparation of landslide susceptibility maps (Zêzere 2002). These factors, which are dependent of the analysis scale and landslide type, generally include: elevation, slope, aspect, plan and profile curvature, topographic wetness factor index (TWI), topographic position index (TPI), slope over area ratio (SOAR), solar radiation, faulting, lithology, lithological layers tilt, precipitation, streams, land-use patterns, normalized difference vegetation index (NDVI) or vegetation density factor, grain size, and spring presence (Van Westen *et al.*, 2008; Reichenbach *et al.,* 2018; Pereira *et al.,* 2020). When related to susceptibility assessments of sea cliffs, landslide-conditioning factors also include cliff edge height and coastal slope toe protection (Marques *et al.,* 2011, 2013; Marques 2018; Guilham *et al.,* 2018; Letortu *et al.*, 2019; Queiroz and Marques 2019). In this study, we followed the classification of Cruden and Varnes (1996), Varnes (1978), WP/WLI (1993), and Dikau *et al.* (1996) to differentiate the types of landslides that may occur in coastal cliffs: falls, slides, topples, lateral spreads, and flows. Identifying landslide types remains challenging, even when supported by intensive fieldwork, which often faces the lack of clear evidence associated with the degradation of landslide features or inaccessibility to cliff faces (Neves *et al.,* 2012). Datasets of aerial photographs can be used to overcome these limitations (Oliveira *et al.,* 2017). Multiple bivariate and multivariate statistical models are used to analyse landslide susceptibility, and most of these models require a subdivision of territory into terrain units and the selection of the appropriate type of terrain mapping units (e.g. grid cells, slope units, geo-hydrological units, unique condition units, and administrative units [Van Den Eeckhaut *et al.*, 2009; Marques *et al.,* 2011, 2013; Epifânio 2014; Corominas *et al.,* 2014; Zêzere *et al.,* 2017]).

Data-driven approaches are the most commonly used for landslide susceptibility and hazard zonation (Kanungo *et al.*, 2006; Girma *et al.*, 2015; Hamza and Raghuvanshi 2017; Mengistu *et al.*, 2019; Shano *et al.*, 2020) whereas other approaches, such as bivariate, multivariate, and active learning statistical methods, are also suitable for assessing susceptibility (Corominas *et al.,* 2014). Bivariate statistical methods use inductive logic, which assumes that the combination of conditions pertaining to various conditioning factors, analysed separately, may lead to landslide prediction in a given area. The evaluation of conditioning factors and their relationship with past landslides in the study area forms the basis for the prediction of places where future landslides may occur (Varnes *et al.*, 1984; Van Westen *et al.*, 1997; Dai *et al.,* 2002; Lan *et al.,* 2004; Girma *et al.,* 2015; Chimidi *et al.,* 2017; Shano *et al.,* 2020).

The information value (IV) method (Yin and Yan 1988), is considered appropriate for evaluating landslide susceptibility (Corominas *et al.*, 2014). It has been widely used worldwide with different geomorphological backgrounds (Yin and Yan 1988; Jade and Sarkar 1993; Lin and Tung 2003; Yalcin 2008; Balasubramani and Kumaraswamy 2013; Zêzere *et al.,* 2017; Mengistu *et al.,* 2019). The IV model is based on the weighted presence or absence of drivers of slope instability. Thus, the landslide density for conditioning factor classes can be determined by overlaying maps of both conditioning factors and inventoried landslides (Mengistu *et al.,* 2019; Shano *et al.,* 2020). If the resulting IV is positive, the causative factor class represents a strong interdependence with landslides in the area (Yin and Yan 1988; Shano *et al.*, 2020), and the weighted value of a conditioning factor class can be represented as the natural logarithm of the landslide density in a factor class divided by the landslide density in the total map area (Van Westen *et al.*, 1997; Shano *et al.*, 2020).

Validation of the landslide susceptibility map is essential for evaluating the predictive capacity of the model. It can be considered as a test of the model's ability to reflect the real environment trough and evaluate its accuracy and predictive capacity (Beguería 2006; Frattini *et al.*, 2010; Shano *et al.*, 2020; Mateus *et al.*, 2021). The receiver operator characteristic (ROC) is a recognised technique used in statistical approach validations to check the performance of the prediction ability of bivariate methods (Shano *et al.*, 2020). This represents a plot of the probability of correctly identified landslides against the probability of incorrectly identified landslides (Gorsevski *et al.,* 2006a; Shano *et al.*, 2020).

However, the dynamics of the Essaouira coastal area have been poorly studied. A beach granulometric technical study was conducted in Essaouira Bay in 1955 by the hydraulic laboratory of Neyrpic (El Mimouni and Daoudi 2012). Other studies have focused on the general morphology of sandy dunes in the upper part of the beach and on the mainland (Gentile 1997; Simon 2000; Lharti *et al.*, 2006). Alternatively, this study aims to: i) define the type and emplacement of each landslide by an inventory validated using a field survey; ii) identify the most important predisposing variables that control the spatial distribution of different landslide types; iii) set and weight the different conditioning factors by applying the IV statistical method; iv) assess landslide susceptibility in Essaouira coastal cliffs for different landslide types and classify susceptible areas to the occurrence of landslides; and v) validate the susceptibility map.

2. Study Area

The Essaouira coastal area is located along the middle of the Atlantic coast of Morocco (Fig. 1) and extends over 134 km. It has high coastal system diversity, including estuaries, bays, beaches, sandy spits, cliffs, and rocky shore platforms (Weisrock 1980; Simon 2000; Lharti *et al.*, 2006). A classification was applied based on three subsystems: sandy coast, rocky coast, and anthropic coast. The study site (Fig. 1) is characterised by stretches of sandy coast (48%), rocky coast (51%), and anthropic coast (1%, the Port of Essaouira), delimited to the north by the Tensift estuary, to the south by Timzguida Ouftas village, to the east by Essaouira province municipalities, and to the west by the Atlantic Ocean and the island of Mogador in front of Essaouira City (Fig. 1). This coastal area has a predominantly semi-natural landscape which is locally interrupted by heavily anthropized coastal areas, particularly in Essaouira City (Fig. 1).

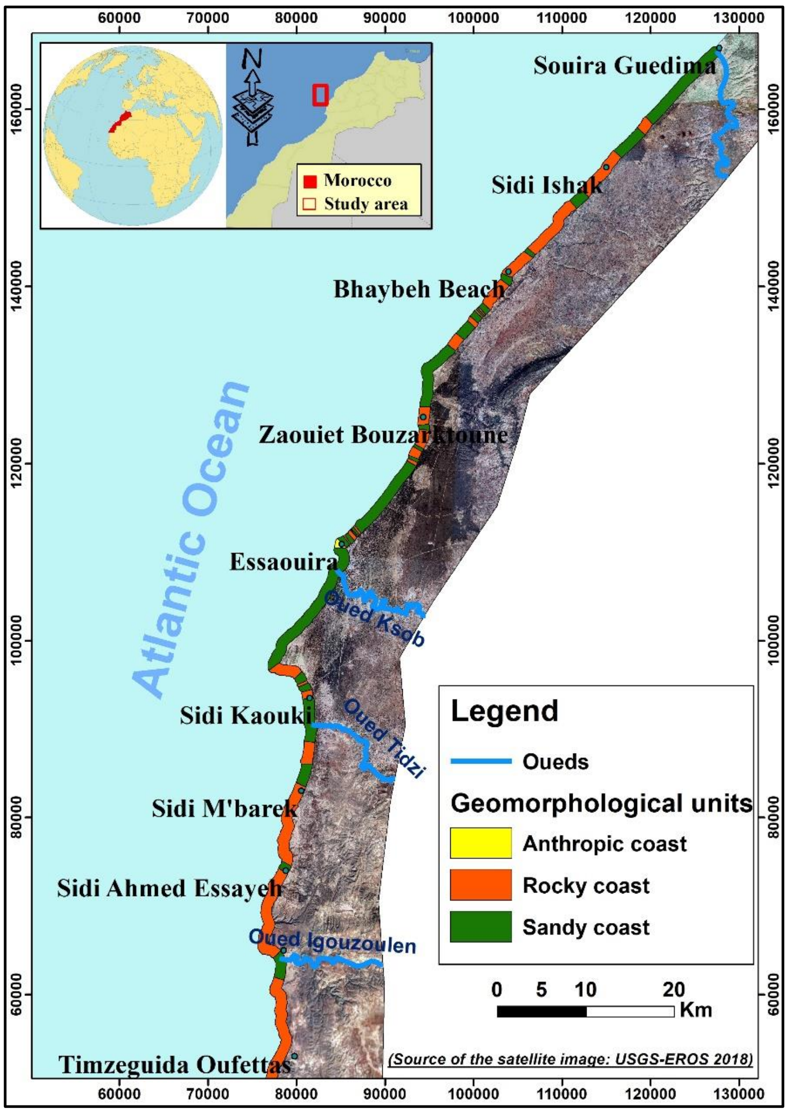

Fig. 1: Geographic location of Essaouira coastal area and its sandy and rocky coast subsystems (Coordinate systems: Lambert Zone I projection)

Geologically, the study area is located in the Atlantic Atlas, which is considered to be the westernmost part of the High Atlas Mountains (Weisrock 1980), with its northern and largest plateau (Haha and Chiadma) dropping gently from SE to NW, in accordance with the overall structural framework. However, the landscape is varied, crossed by cuestas and vigorous crests, turned towards the SE, and associated with the frequent alternations of sandstone, dolomitic, limestone, marl, clay, and gypsum layers. The landscape is interrupted by sudden isolated anticlinal folds, such as the Jbel Hadid (725 m high), to the north, or the Jbel Ouamsitten (900 m high) to the south. Towards the west, the abundance of consolidated dunes and sandstones with oblique stratification and conglomeratic levels is relevant (Weisrock 1980). To the south, a coastal basin with original sedimentary material known as the "Haha Basin" (Dufaud *et al.*, 1966) is associated with the opening of the North Atlantic, which is generally consistent with the end of the Triassic (Choubert *et al*., 1971; Hallam 1971; Le Pichón 1971; Weisrock 1980). It consists mainly of sandstones, pelites, conglomerates, and red salt clays, with essentially continental facies. Deep marine sedimentation was successful from the Lower Liassic to the Upper Cretaceous. During these long periods, the sedimentation of the coastal basin constantly oscillated between an epicontinental regime, with terrigenous deltaic or alluvial contributions and marine organogenic or evaporitic deposits, and a more open marine regime with neritic limestones and marls. Towards the north, the coastal platform is largely developed, also called the "Moghrebian platform", from the name attributed to the sandy and sandstone deposits that cover it (Choubert and Ambrogi 1953; Weisrock 1980), and thus tapers off at the southern mountainous part.

From a structural point of view, the study area is characterised by a double structural division marked by a close adaptation to the hydrographic network (Weisrock 1980). The first one is linked to the opening of the Atlantic, including the extensional faults fundamentally oriented NNE-SSW, for the entire Atlantic Atlas and its northern edge. This second direction may have the same origin as the first; these Hercynian breaks in the basement influenced sedimentation and then reappeared, affecting the cover during the Atlasic phases (Saadi 1972). This second direction, WNW-ESE, related to the opening of the Atlantic, is increasingly evident (Oued Ksob, northern fallout anticlines, Oued Tensift). This direction is attenuated towards the S, while in the central region (Tamanar Plateau), a W-E direction appears as a result of the ancient Hercynian direction (Saadi 1972). In addition to these two fundamental systems and because of the thickness of the saliferous clay layer, the Essaouira region is marked by the development of diapiric-style tectonics, well represented particularly in the SE of Essaouira (Weisrock 1980).

From a geomorphological point of view, landform distribution in the study area is asymmetrical: all the plateaus dominate to the N and NW sectors, and are almost absent to the S and SE, occupied by the mountain. In accordance with the general layout of the High Atlas, the altitudes increase towards the south and east. Thus, the morphogenesis of the Atlantic Atlas depends on general physical geography, in addition to the structural morphology of the folded chains, the phenomena of encrustation, coastal eolian constructions, and glaciation (Weisrock 1980). The Atlantic Atlas is open to oceanic influences. This area is particularly characterised by its dual character as a mountainous and coastal region, which makes it possible to link continental and marine morphology; the latter offers the advantage of being able to establish a solid chronological base from the Pliocene onwards by comprising a whole series of stepped fossil beaches. The coastal area has a uniform appearance from north to south. On average, the Mesozoic bedrock disappears under a sandy cover shaped into innumerable encrusted hills along the ocean (Weisrock 1980).

From a hydrological point of view, the presence of two large watersheds, Oued Tensift and Oued Ksob, were noted, to which coastal Oueds are added: Oued Tidzi and Oued Igouzoullen. These hydrographic networks are an important source of sediment supply and are characterised by a flow which is roughly carried out from E to W, rather faithfully adapted to the topographic framework; however, the courses of the valleys, more often monoclinal or orthoclinal than cataclinal, reveal a long evolution and successive re-adaptations (Weisrock 1980).

The Essaouira cliffed coastal sector is characterised by the presence of multiple landslide types, which are the dominant hazards responsible for the constraints of human activities and safe land use (Moore and Griggs 2002). The seismic context shows that the coast between Safi and Essaouira has landslide activity that is likely related to seismic events (Elmrabet *et al.,* 1989). The most significant of which, capable of causing disproportionate effects on a highly unstable cliff, occurred in 1757, on 7th March 1930 (32° N, 11.5° W, M = 5.1, felt in Casablanca, Safi and Essaouira, intensity IV), and on 2nd August 1963 (34.7° N, 8.9° W, M = 4.1, felt in Casablanca and Mohammedia, intensity IV). In the 1757 event, the landslide could also have been conditioned by an aftershock of the earthquake on 1st November 1755 affecting the natural instability of the cliff, which had been enhanced by the effects of the tidal wave (Elmrabet *et al.,* 1989).

Climatically, the Atlantic Atlas is located at a relatively low latitude (approximately 31° parallel), which places it under the predominant influence of subtropical anticyclonic cells at the limit of the great displacements of polar air masses. It is a position sensitive to the slightest deviations of these centres of action; thus, it is particularly interesting to reconstitute the possible conditions of past climatic oscillations identified by their morphogenetic marks (Weisrock 1980).

The Essaouira province is characterised by a steppe climate of type BSh according to the Köppen-Geiger classification, with low rainfall, an average annual temperature in Essaouira city of 18.7 °C, and average annual rainfall of 295 mm (Climate-data.org). The dominant climate in the Essaouira region is semi-arid with diverse temperature and precipitation values. This is because of the oceanic (Atlantic) setting on one side and the height of the mountains on the other. The Essaouira region is an area where hot summer and humid winter winds change. The "Chergui" (the hot wind from the Sahara), the northeast wind that blows almost all year round. It is characterised by a mild climate throughout the year. The average temperatures are 16.4 ºC in January and 22.5 ºC in August. The annual rainfall is approximately 280 mm. Two main seasons can be distinguished: i) the wet season that includes winter and autumn, with a monthly maximum fluctuating between December and November. Precipitation peaks are clearly marked in autumn and winter, before gradually decreasing from February to May, and ii) the dry season from April to September. This season is characterised by scarce rainfall. July and August are the driest months throughout the year, with almost no rainfall. Regarding the spatial distribution, both the precipitation and humidity are higher in the coastal zone, and they are always > 75%. Summer fog is particularly important in Essaouira and other sites that are exposed to maritime influences (Hander 1988).

Using the rainfall data from stations of Adamna, Chichaoua, Talmest, Abadla, and Igrounzar, which were provided to us by the Tensift Water Basin Agency, the average monthly variability of rainfall was analysed for the period 1965–2015, and results show the existence of a rainy season between October and April with a maximum in March for the Abadla and Chichaoua stations and a maximum in December and November for the Talmest, Igrounzar, and Adamna stations. The dry season extends between June and September, with the lowest rainfall recorded in July and August. The monthly variation in rainfall showed an average of 15.3 mm for Chichaoua and 14.4 mm for Abadla. Rainfall was similar over the same period for Chichaoua and Abadla. The values observed from October to April exceeded the average rainfall for each of these two stations, with a maximum in March (27 mm) and a minimum in July (0.5 mm) and August (1 mm). Thus, the evolution of monthly precipitation was the same at these two stations. It argues in favour of a simple hydrological regime characterised by a regular annual alternation of high and low water. The monthly rainfall at the three stations Adamna, Talmest, and Igrounzar showed that the maximum rainfall was recorded in November and December, while the average rainfall was approximately 20 mm for Igrounzar and Talmest and 26 mm for Adamna.

Regarding the annual variations in rainfall at the five stations, the Adamna, Igrounzar, and Talmest stations have mean annual rainfall of 322 mm, 229.1 mm, and 255.4 mm, respectively. At the Adamna station, there were several rainy years with values that greatly exceeded the interannual average, namely 1987/88, 1988/89, 1994/95 to 1996/97, 2008/09 to 2010/11, with a maximum rainfall of approximately 718 mm in 1995/96 and a minimum of approximately 136 mm in 2006/06. For the Igrounzar station, the highest rainfall was observed during 1987/88, 1988/89, 1994/95 to 1996/97, 2008/09, and 2009/10. However, the least rainy years were: 1968/69, 1976/77, 1991/92, and 2014/15. For the Talmest station, the wettest year was 1995/96 with 559.5 mm and the driest year was 2014/15. For this station, we did not have data for the years 1971/72 until 1975–76.

From a hydrogeological point of view, the Essaouira Basin and its coastal zone constitute a set of independent but very similar hydrogeological systems that correspond to synclinal basins. Groundwater exists only in localised areas within these systems. Water generally circulates at depth in different limestone or sandstone levels by karstic pathways and comes out in the form of springs at low points in contact with an impermeable clay or marl level (Cochet and Combe 1975). The combination of the effects of tectonics and diapirism has caused the compartmentalisation of the basin into several aquifer systems.

For example, the piezometry of the Plio-Quaternary aquifer shows an overall flow direction from E-SE to W-NW, conditioned by the straightening of its bedrock to the east following the uplift of the Tidzi diapir (Mennani 2001). There are significant fluctuations between periods of high and low water (Fekri 1993; Mennani 2001; Bahir *et al.*, 2002; Bahir *et al.*, 2017), which are related to precipitation which thus controls the regime of the phreatic aquifer. Several problems related to water scarcity and long recurrent periods of drought have been observed in the Essaouira region in recent decades (Bahir *et al.*, 2002; Chkir *et al.*, 2008; Chamchati and Bahir 2013; Bahir *et al.*, 2017). For this reason, the piezometric level in the study area tends to decline with the inability of some other wells to recover their initial water level, aggravated by the combined effect of the year 1995, the driest year that Morocco experienced during the 20th century (Bahir *et al.*, 2002), and overexploitation (Chkir *et al.*, 2008; Bahir et *al.*, 2017).

3. Methodology

The current research used different data sources for landslide susceptibility analysis, and their preparation was supported by field surveys and validation. The methodological steps considered for training and validation of the coastal landslide susceptibility models are shown in Fig. 2 and follow this sequence: i) elaborate the landslide inventory, classifying the landslides by type and depth of the rupture surface (shallow and deep); ii) prepare a set of 22 conditioning factors grouped into 7 categories (topographical, geomorphological, lithological, geotechnical, hydrological, climatic, and tectonic); iii) model coastal landslide susceptibility using the IV method for the Essaouira coastal area, using pixels and elementary terrain units (ETUs); and iv) independently validate the predictive susceptibility models using ROC curves and area under the curve (AUC).

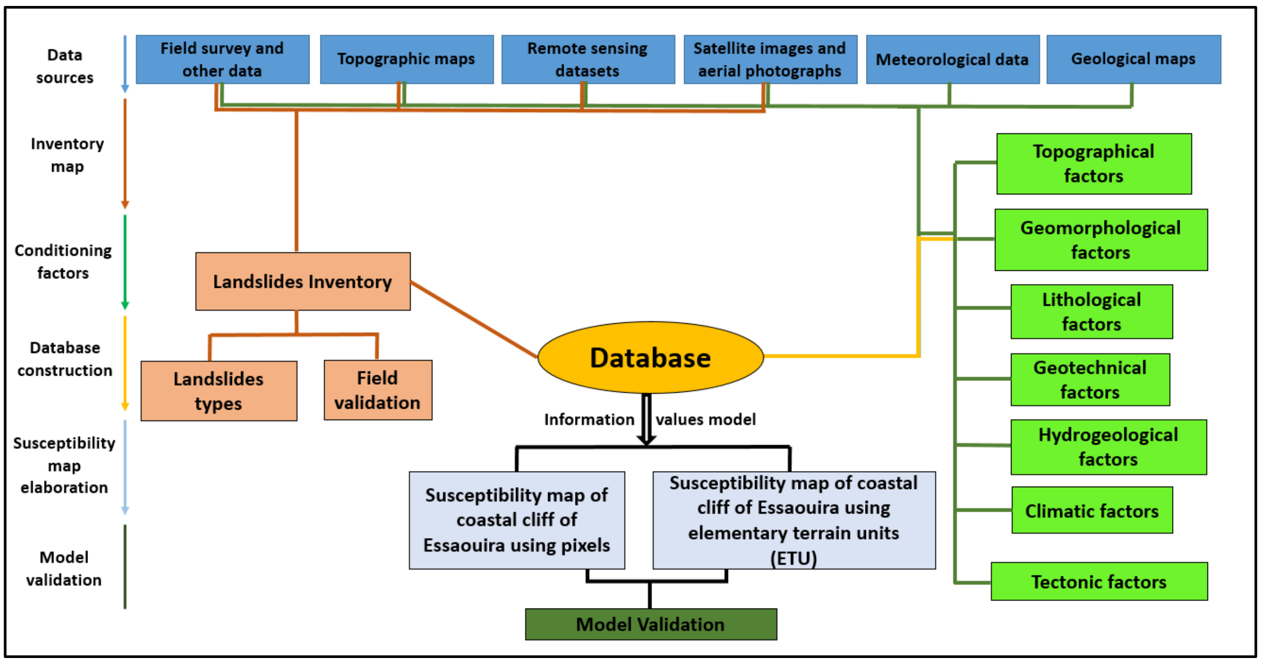

Fig. 2: Schematic of the methodology used

Coastal systems were classified into sandy and rocky subsystems according to morphometric and operational criteria, and the ETU was defined based on the methodology proposed by Marques *et al.* (2011); the upper and lower limits of the terrain units were defined by the bottom and the top of the cliff, respectively, while the lateral limits were geometrically drawn perpendicular to the contour lines of the topography and defined by the segmentation of the ridge line into 50 m wide sections. In total, there were 1534 terrain units on the rocky coast. Each terrain unit was classified as stable or unstable based on the quantification of the percentage of unstable area of each slope unit.

3.1. Landslide inventory

The most essential part of the landslide susceptibility assessment framework is the landslide inventory, which includes the identification of their location, size, type, and depth to understand the relationship between landslide occurrence and the dataset of predisposing factors (Ercanoglu and Gokceoglu 2004; van Westen *et al.,* 2006; Petley

2008; Epifânio *et al.*, 2013). The landslide inventory was of the historical type, with no past date of occurrence limits, and was based on the interpretation of different data sources covering the entire study area (Table 1), such as historical records, 10 m resolution Sentinel satellite imagery, high-resolution ortho-imagery analysis, and intensive field investigation.

Table 1: Data sources table

Data type	Data denomination	Source	Scale / resolution / Duration
Topographic maps	Sidi Ishaq 2008	National Agency of Land Conservation, Cadastre and Cartography (ANCFCC)	1/25000
	Berrakat Erradi 2008		
	Sebt Akermoud 2008		
	Bir Kaouat 2008		
	Moulay Bouzarqtoune 2008		
	Jbel lahdid 2008		
	Essaouira 2008		
	Chicht 2008		
	Ras Sim 2008		
	Essaouira El Jadida 2008		
	Sidi Kaouki 2008		
	Tidzi 2008		
	Sidi Ahmed Essayeh 2009		
	Tafdna 2009		
Geological maps	Tamanar map	Ministry of Energy and Mines, Water and Sustainable Development	1/100000
	Taghazout map		1/100000
	Marrakech map		1/500000
Aerial photographs	Mission TAMANAR 07/2016	National Agency of Land Conservation, Cadastre and Cartography (ANCFCC)	1/7500
Meteorological data	Adamna station	Hydraulic basin agency of Tensift (ABHT)	1977–2015
	Igrounzar station		1968–2015
	Talmest station		1984–2015
	Chichaoua station		1965–2014
	Abadla station		1969–2014
Satellite images	Sentinel	https://scihub.copernicus.eu/ (Copernicus 2021)	10 m
	High resolution Ortho-imagery	https://earthexplorer.usgs.gov/ (USGS-EROS 2018)	0.3 m
	Digital elevation model	https://search.asf.alaska.edu/ (JAXA/METI 2020)	12.5 m

The identification of the landslides was based on the interpretation of their specific morphological features that are noticeable in high-resolution imagery, including the crown, main scarp, flanks, body, and toe (Pawluszek 2019). Other features include the presence of flow materials along gullies, streams with different erosional features, flow tracks, scars along the cliff face, and block deposits on the cliff base (Epifânio *et al.*, 2013; Elkadiri *et al.*, 2014). In addition, extensive field observations were used to validate the inventory and add new landslides that were not observed in satellite images or identified in other data sources.

3.2. Conditioning factors

Conditioning factors describe terrain conditions that are directly or indirectly associated with landslide occurrence and are essential for landslide susceptibility mapping based on data-driven methodologies. Different types of variables (conditioning factors) were compiled and/or generated in a GIS for susceptibility analysis. According to Marques *et al.* (2011, 2013), all conditioning factors influencing the stability of coastal cliffs and slopes should be considered because they may contribute to predicting the spatial occurrence of future instability. Notably, the selection of conditioning factors associated with these processes appears to be a difficult task because these factors typically work in combination in a multivariate system (Epifânio *et al.,* 2013; Reichenbach *et al.,* 2018).

Based on geomorphological characteristics, bibliography, and field surveys, 22 landslide conditioning factors were selected for the study area. From these, 10 conditioning factors were computed from a freely available digital elevation model (ALOS PALSAR RTC DEM) with a 12.5 m resolution (source: https://search.asf.alaska.edu/): elevation, slope angle, slope aspect, slope plan curvature, slope profile curvature, cliff height (calculated by the average of top pixels in each ETU), topographic wetness index, topographic position index (classified considering the distance of SD to the mean value for both sides of the distribution), slope over area ratio (using a base 10 logarithmic progression of class limits), and solar radiation (Table 2).

Solar radiation was used as a proxy variable for slope aspect because it enables the quantification of the weight of trivial qualitative quadrants (Epifânio *et al.,* 2013). Slope angle is the most important predisposing factor for the occurrence of landslides (Mancini *et al.*, 2010); however, in our study area, the slope angle does not have the same importance for all landslide types, and plan and profile curvatures can be associated with the acceleration and deceleration of the flow, as well as the convergence or divergence of the flow, and can influence the local drainage systems and the kinematics of landslides (Mancini *et al.*, 2010).

The land use map and the NDVI were extracted from Sentinel images 2021 (10 m resolution, Table 1). The lithology, toe lithology, and faulting data were obtained from the compilation of a bibliographical review and from three digitised geological maps: Tamanar and Taghazout 1/100000-scale in the southern section, and Marrakech 1/500000-scale for the northern section, completed with the field survey.

Meteorological data and historical rainfall records were used for extracting the rainfall factor using the arithmetic mean method (Smaij, 2011), which consists of calculating the annual arithmetic mean of the values obtained at the weather stations and projecting them using inverse distance weighting interpolation. Field surveys, topographic maps (1:10,000), and digital elevation models (DEM) were used to identify and map the stream networks. The presence and type of cliff toe protection, lithology tilting, and the presence of springs were extracted from satellite image observations and field surveys.

Field work revealed that most landslides occur above weak or friable layers, making geotechnical properties a factor to account for. Moreover, the grain size was added to the variable list after data extraction from 16 samples using the BetterSize Lazer Particle Size Analyser 9300S (Table 2). The grain sizes of clay, silt, and sand (Table 2) were spatially identified as the same predisposing factors. The sampling sites are shown in Fig. 6 (red arrows). Organic matter content analysis was also applied to the samples using the loss on ignition (LOI) method (Heiri *et al.* 2001), as an important factor that has a strong relationship with the presence of vegetal cover (Table 2), which indicates that the presence of water promotes the occurrence of landslides.

Table 2: Input conditioning factors

Conditioning Factor	Number of classes	Minimum value	Maximum value	Variable Type
Elevation (m)	13	0	261	numerical
Aspect	10 or 9	Flat (−1)	North 337.5–22.5°	numerical
Slope (°)	11	0	75	numerical
Curvature profile	3	-17.81 (concave)	21.1 (convex)	numerical
Curvature plan	3	-9.82 (convergent)	11.35 (divergent)	numerical
Height (m)	13	0	254	numerical
TPI	6	-88	69.37	numerical
TWI	6	-1.55	29.35	numerical
SOAR	6	0	4.72	numerical
Solar radiation (kWh/m2)	6	400	1000	numerical
Land-use	6	Bare ground, Light vegetation, Breakwater area, Dense vegetation, Cultivated areas, Roads and habitation		categorical
NDVI	5	Water, Bare soil, Sparse vegetation, Moderate vegetation, Dense vegetation		categorical
Layers tilt	2	Towards sea tilting, Sub horizontal tilting		categorical
Grain size clay (% Clays < 2 µm)	6	3	35	numerical
Grain size silt (% Silt 2 µm < 63 µm)	6	6	72	numerical
Grain size sand (% Sand 63 µm < 2 mm)	6	0	91	numerical
Organic matter (LOI%)	6	0.94	7.41	numerical
Precipitation (mm)	5	252	306	numerical
Drains network	2	0	1	categorical
Spring	2	0	1	categorical
Faulting	2	0	1	categorical

Lithology	20	See the results section	categorical
Toe lithology	5	Grey marls, Marley limestones, Essaouira sandstone, Dolomitic sandstone, Dolomitic limestones	categorical
Toe Protection	4	Rock platform protection, Slope deposit protection, Beach protection, No protection	categorical

3.3 Susceptibility modelling and validation

The method used to evaluate the susceptibility to the occurrence of coastal landslides is the IV (Yin and Yan 1988; Zêzere 2002), which is a bivariate statistical method particularly suited to study relationships between the dependent variable (landslides) and the set of independent conditioning factors. This method has been successfully applied in coastal areas worldwide (Marques *et al.*, 2011, 2013; Epifâneo *et al.*, 2013, 2014).

Using this bivariate statistical method, it is possible to weight each class of each predisposition factor of slope instability in an objective and quantified manner.

The IV score (Ii) for any class Xi of an independent variable (X) was determined for each landslide type Y using the following equation:

$$\mathbf{Ii = ln\frac{\mathit{Si/Ni}}{\mathit{S/N}}} \qquad \mathbf{(1)}$$

Where:

- Si = nº of cells with landslides and variable Xi in Essaouira coastal area;
- Ni = nº of cells with variable Xi in the Essaouira coastal area;
- S = total nº of cells with landslides in the Essaouira coastal area;
- N = total nº of cells in the Essaouira coastal area.

When a class of conditioning factors does not have registers of landslides (Si = 0), the Ii score is not calculated because of the impossibility of logarithmic normalisation, and it is assumed that that class has an Ii score lower than the minimum registered. For example, the minimum IV index was -5.7014031 for slope aspect Class 1 (flat areas) for deep translational slides; therefore, we took -5.702 for variable classes without any landslide.

The final value of susceptibility to landslides calculated for each cell j corresponds to the sum of the Ii scores present in that unit, given by the following equation:

$$\mathbf{Ij = \sum_{i=1}^{m} \mathit{XijIi}} \qquad \mathbf{(2)}$$

Where:

- m = number of variables;

› Xij is equal to 1 or 0, depending on whether variable Xi is present in cell j.

To assess coastal landslide susceptibility, 15 predictive models were individually developed for each inventoried landslide type in this coastal area, considering the landslide partitions defined in Table 3, and the standard model procedures defined in Section 3. Table 3 shows the 15 different landslide partitions according to the landslide type used for assessing landslide susceptibility: total landslides, deep landslides, shallow landslides, deep rotational slides, shallow rotational slides, deep translational slides, shallow translational slides, rock topples, rock falls, rock slides, debris falls, debris flows, and debris slides. With these landslide dataset partitions, we expect to better understand the drivers responsible for the occurrence of different landslide types in this coastal area. Each landslide-type inventory dataset was then subdivided into training and validation groups (Remondo *et al.*, 2003). The training group containing 70% of the inventory was used in the model building and the validation group containing 30% of the inventory was used to conduct an independent cross validation process over the model first results; the 70/30 partition was selected randomly, because it agrees with the commonly used partitions used for landslide susceptibility model training and validation (Chen *et al.*, 2020). We also adopted a sensitive approach to eliminate some landslide conditioning factors that have little or no contribution to landslide occurrence based on the IV score results.

Additionally, to assess the importance of the representativeness of the inventory, susceptibility modelling was also considered for some landslide types, splitting them into two subgroups considering the depth of the rupture surface: shallow and deep-seated for rotational and translational slide types.

Table 3: Predictive susceptibility model strategy and landslide inventory dataset partitions

Model ID	**Description of the landslide partition dataset used for assess susceptibility**	**Training – 70%**			**Validating – 30%**		
		Area	**Slides number**	**ETU number**	**Area**	**Slides number**	**ETU number**
Model 1	All landslides (no landslide type or depth of the rupture surface differentiation)	3149643	412	682	1349847	176	292
Model 2	Deep-seated landslides (no landslide type differentiation)	2570471	92	371	1101630	40	159
Model 3	Shallow landslides (no landslide type differentiation)	208086	75	180	89180	32	77
Model 4	Rotational slides (no depth of the rupture surface differentiation)	553238	100	281	237102	43	120
Model 5	Deep-seated rotational slides	490737	67	207	210316	29	89
Model 6	Shallow rotational slides	64840	34	74	27789	14	32
Model 7	Translational slides (no depth of the rupture surface differentiation)	2222341	67	270	952432	29	116

Model 8	Deep-seated translational slides	2082644	26	165	892562	11	71
Model 9	Shallow translational slides	143551	41	106	61522	18	45
Model 10	Rock topple (source areas)	41086	85	136	17608	36	58
Model 11	Rock fall (source areas)	175529	104	219	75227	45	94
Model 12	Rock slides	21920	11	26	9394	5	11
Model 13	Debris fall (source areas)	39314	4	21	16849	2	9
Model 14	Debris flow (source areas)	204500	33	67	87643	14	29
Model 15	Debris slide	14206	8	20	6088	3	8

For the pixel terrain unit approach, susceptibility was assessed for the different landslide types, and all dependent and independent variables were transformed into a spatial grid database with 12.5 × 12.5 m resolution following the DEM pixel size, and all the data were projected in the Lambert conformal conic Zone 1 coordinate system with Merchich datum.

For the ETU approach, to assess landslide susceptibility, the application of any statistical method requires partitioning the study area into smaller terrain units. In the present study, the main modelling was developed on a pixel-based model, and the conditioning factor layers were transformed into ETUs, considering the weight of each factor in each ETU, in order to apply the terrain unit method and compare the two approaches (pixel and ETU).

However, susceptibility results are harmonised in ETUs. The ETU use is done because i) they have a strong relationship with the morphology and geometry of the system that we are trying to model; ii) they are fitting to the most used land-use planning formats as they are mostly vector approaches and system-based, either that as a physical system or a human settlement; and iii) they are also a factor of uniformity and help deal with heterogeneous data (Calvello *et al.*, 2015). Additionally, for planning purposes, it is easier to clearly identify the ETU in the territory when compared to pixels.

4. Results and discussion

4.1. Landslides in cliffs and coastal slopes of Essaouira

The detected landslides were assigned according to the classifications of Varnes (1978), WP/WLI (1993), Cruden and Varnes (1996), and Dikau *et al.* (1996), and 10 landslide types were identified: debris fall, debris flow, debris slide, rock fall, rock slide, rock topple, deep rotational slide, shallow rotational slide, deep translational slide, and shallow translational slide.

Expert and fieldwork inventory validation allowed landslide limit corrections and the identification of new landslides. Some examples of landslides are shown in Fig. 3.

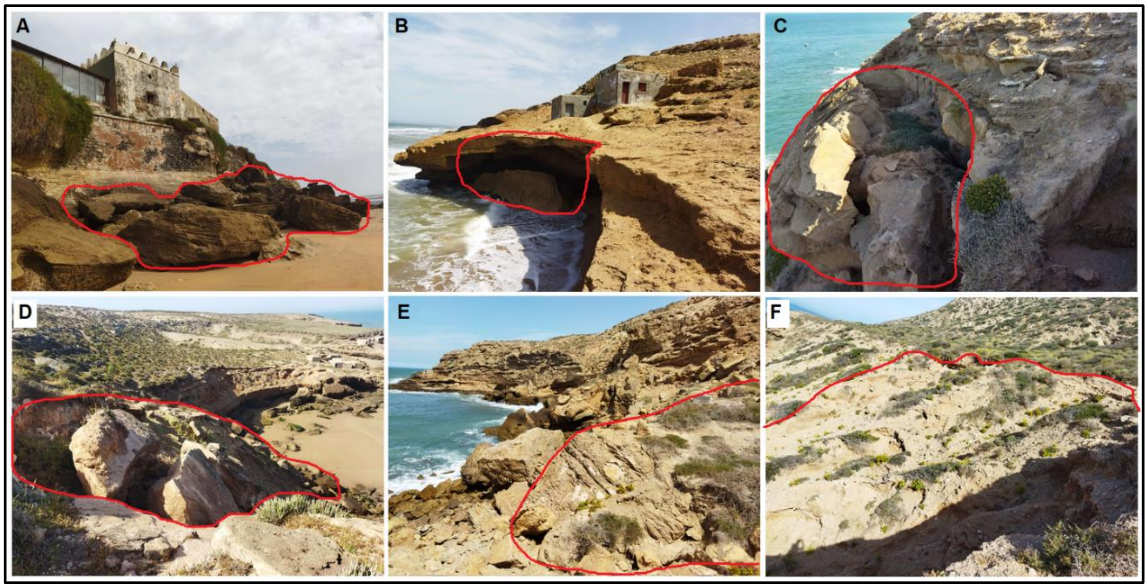

Fig. 3: Some landslide type examples from the study area; A, B: rock falls, C: rock topple, D: translational slide, E: rotational slide with back tilting, and F: debris flow

The final inventory of the study area comprised 588 landslide records (Fig. 4). Rock falls were the most frequent slope instability phenomena in the study area, with 149 records, followed by rotational slides, while the least frequent landslide type was debris fall, with only 6 records. Most of the study area was occupied by translational slides (68%) followed by rotational slides. These landslide types typically have larger areas per landslide, deeper rupture surfaces, and frequently occur along the entire cliff/coastal slope profile.

Slope instability was present along the whole study area, resulting in the identification of 974 ETUs with landslides (63.5%), and 28797 unstable pixels (46.5%).

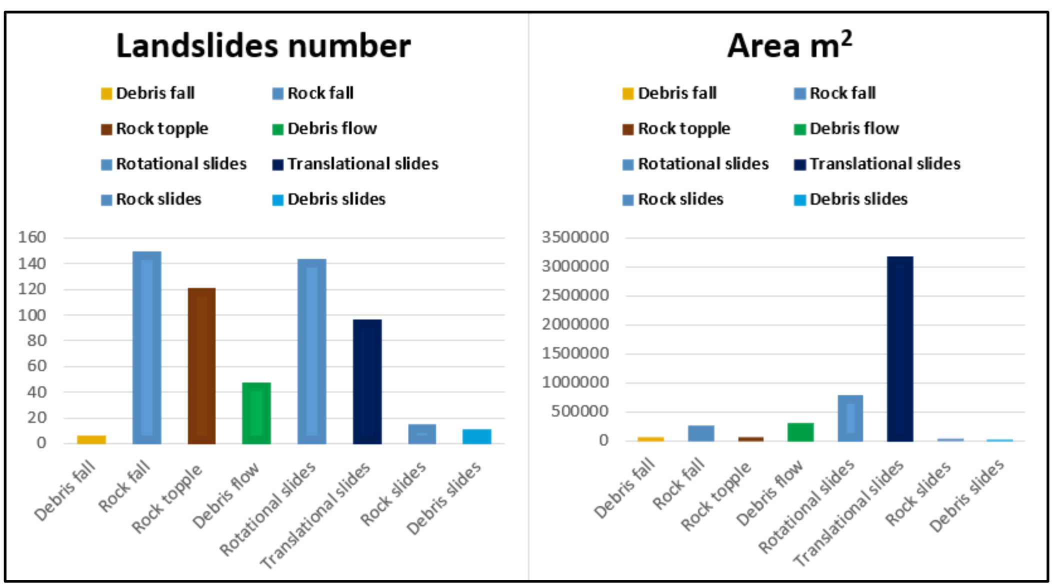

Fig. 4: The relative distribution of landslides by type and area in the ETUs of the study area

Nevertheless, the heterogeneity of the spatial distribution of landslide types (Fig. 5) over the study area was higher in the southern section because of the higher concentrations of rotational and translational slides.

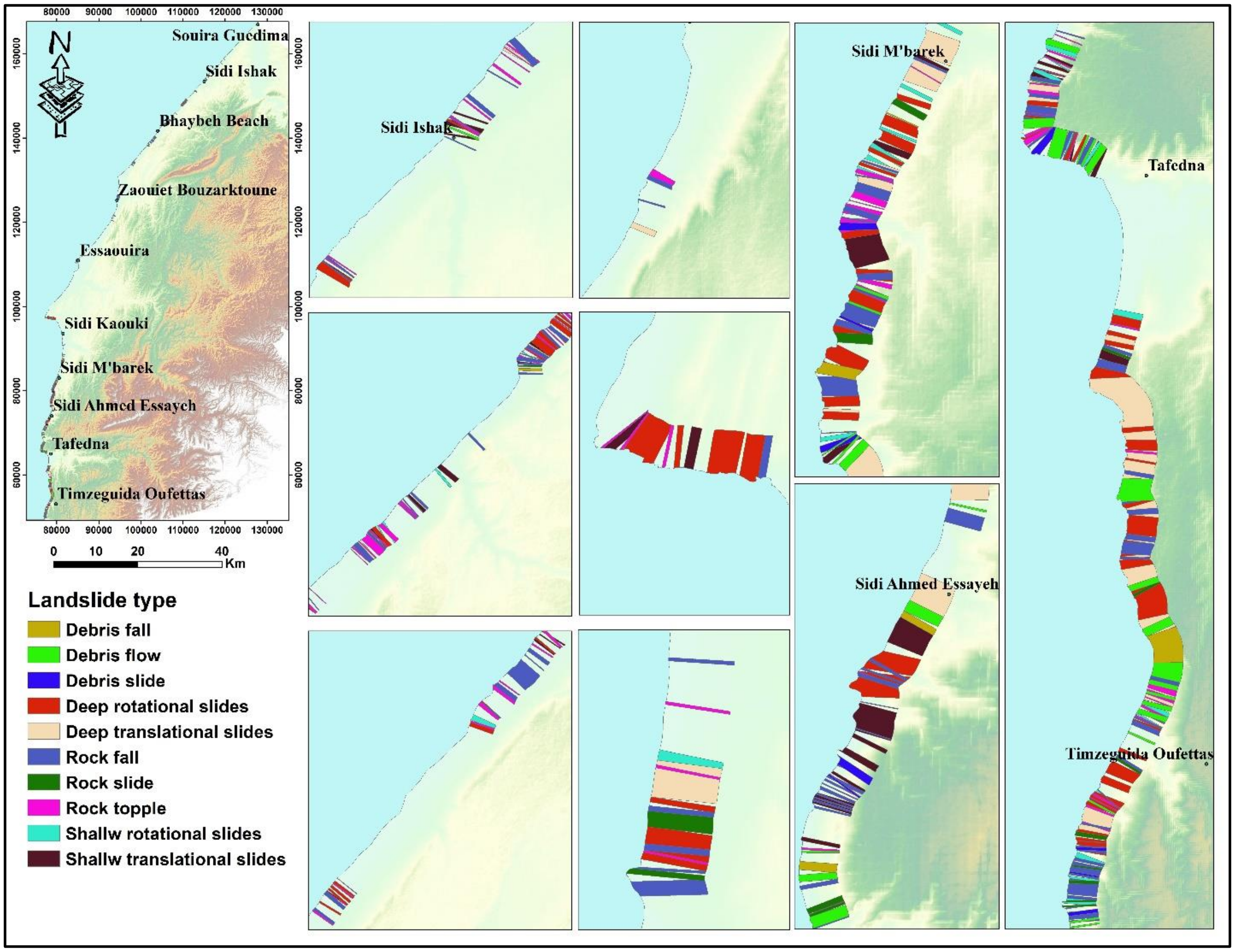

Fig. 5: Spatial distribution of landslide types in the study area

4.2. Driving forces of instability in Essaouira

Lithology, structure, and landslide deposits are important conditioning factors for susceptibility analysis. These can be proxies for permeability, shear strength, and propensity for physical and chemical weathering of rock and soil materials (Varnes 1984, Epifânio *et al.*, 2013). Twenty main lithological units were identified in the study area: (1) calcareous crusting; (2) clay and sandstone; (3) conglomerate and dune sediments; (4) conglomerate with sandy matrix; (5) dolomitic limestones; (6) dolomitic sandstones; (7) dune sandstone with oblique stratification; (8) Essaouira sandstone/calcarenite; (9) friable sandstone layer; (10) grey clays; (11) grey marls; (12) heterogeneous conglomerate; (13) limestone bar; (14) lumachelic clayey limestones; (15) marls; (16) marly limestones; (17) pudding conglomerate; (18) sandstone dolomites; (19) sequence of marls and marly limestone; and (20) terrigenous red deposit (Table 4).

The spatial distribution of the lithological units (Table 4), shows that, in general, limestone units are more frequent in the southern sector, frequently combined with grey marls and clays of the Hauterivian and Aptian (Cretaceous). Calcareous crusting, friable sandstone layers, and terrigenous deposits are found in all coastal areas. The conglomerate and sandstone units are more concentrated in the northern sector, where consolidated dunes can also be found.

Regarding the number of ETUs per lithology type, calcareous crusting and Essaouira Sandstone-calcarenite are the two lithological formations most funded in the majority of ETUs, present in 1216 and 1270 ETUs, respectively. This is because, in the encrustation phenomena, coastal eolian constructions become dominant in the study area as we mentioned in geological settings.

The most lithological formations occupied by the instabilities are: dune sandstone with oblique stratification, friable sandstone layers, grey marls, heterogeneous conglomerate, limestone barre, marls, sequence of marls, and marly limestone.

Table 4: Predominance lithology by area and ETU

Lithology	Predominance area	Number of ETUs	Number of unstable ETUs	% Of unstable ETUs	IV Results
Calcareous crusting	All coastal area	1216	240	19.74	-0.01
Clay and sandstone	Southern coastal area	33	25	75.76	-1.68
Conglomerate and dune	All coastal area	1340	782	58.36	-0.31
Conglomerate with sandy matrix	Northern coastal area	33	3	9.09	-5.70
Dolomitic limestone	Southern coastal area	320	183	57.19	-1.03
Dolomitic sandstones	Southern coastal area	13	4	30.77	-5.70
Dune sandstone with oblique stratification	Southern coastal area	284	243	85.56	0.64
Essaouira sandstone - calcarenite	All coastal area	1270	628	49.45	-1.67
Friable sandstone layers	All coastal area	479	343	71.61	0.39
Grey Clays	Southern coastal area	50	23	46.00	-2.96
Grey Marls	Southern coastal area	229	167	72.93	-1.01
Heterogeneous conglomerate	Southern coastal area	147	119	80.95	1.03
Limestone barre	Southern coastal area	159	154	96.86	0.56
Lumachelic clayey limestone	Southern coastal area	50	32	64.00	0.24

Marls	Southern coastal area	69	60	86.96	0.61
Marly limestone	Southern coastal area	67	63	94.03	0.27
Pudding conglomerate	Northern coastal area	152	33	21.71	-2.23
Sandstone dolomites	Southern coastal area	50	28	56.00	-0.35
Sequence of marls and marly limestone	Southern coastal area	282	275	97.52	0.70
Terrigenous red deposit	All coastal area	48	12	25.00	-1.18

Stratigraphic profiles (Figs. 6 and 7) show detailed lithological changes over the study area and allow for a better understanding of cliff lithological variations and the emplacement of friable layers that have a direct influence on the occurrence of landslides.

In the southern section, a large variation in the lithological units was noted with respect to the spatial distribution; therefore, the majority of stratigraphic logs were concentrated in the southern section (from log 1 to log 13), while there was little variation in the northern section (from log 14 to log 16). Regarding the lithological materials, the presence of friable or weak layers (friable sandstone, sand, clays, and marls) were noted in all logs except logs 3, 7, 9, 13, and 14.

As tilting layers are more favourable to instabilities because of the gravitational forces, the predominant sub-horizontal layering also has a contribution, while the majority of those layers are deposited on weak or friable layers, which are stimulated the instability in multiple locations in the study area referring to the field survey. These friable layers are typically placed between the impermeable or competent layers, which are the result of either the different diagenesis degrees or compaction, or the high clay content according to grain size analysis, which makes them more friable than adjacent layers. According to the field survey, these layers are generally behind the occurrence of numerous landslides, which is why they are considered important, particularly because some of them are in contact with springs and others are in the bottom part of the cliff, which means more lithostatic pressure, and thus more susceptibility to landslide occurrence.

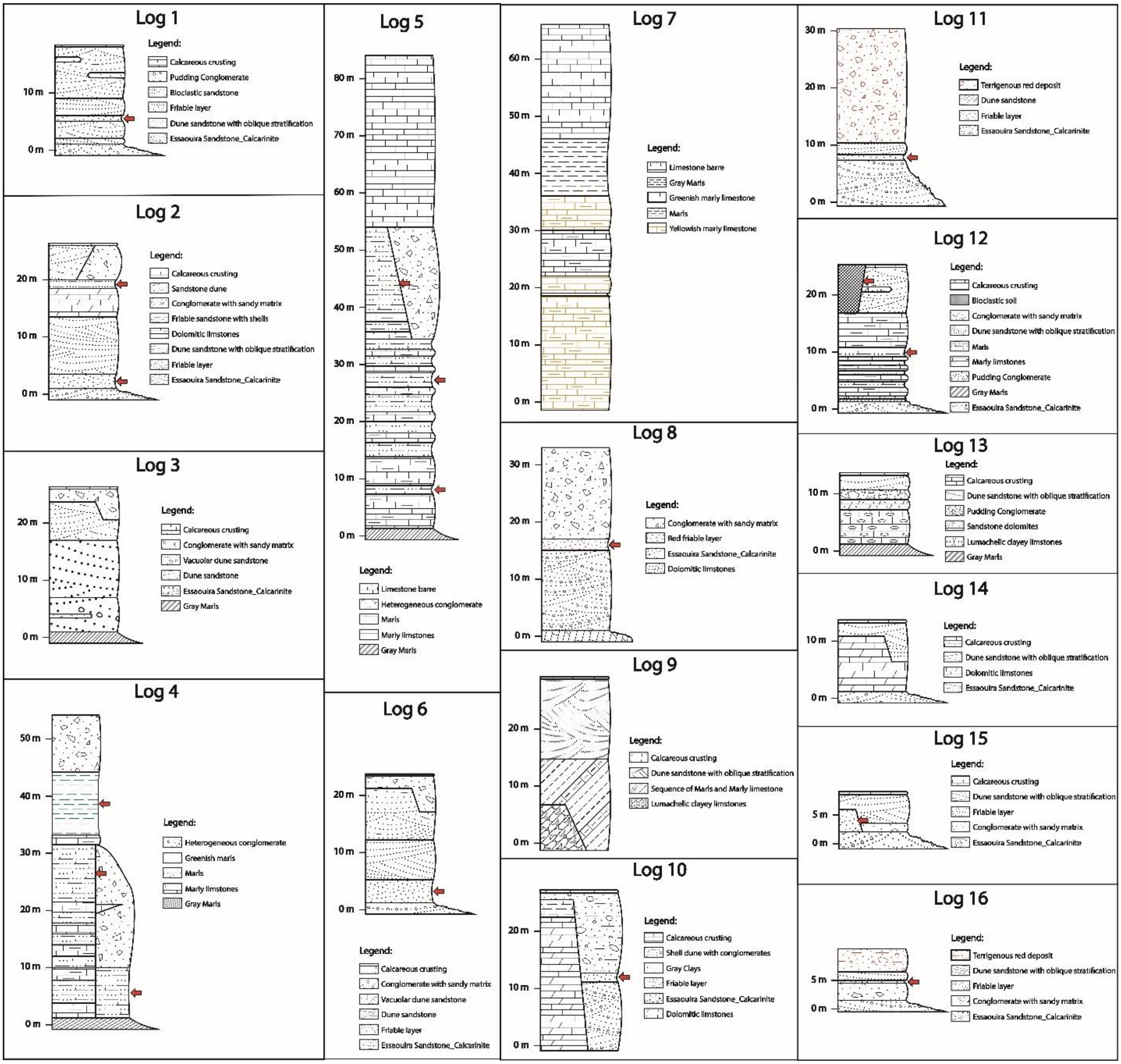

Fig. 6: Stratigraphic columns for the Essaouira coastal area

Elevation is another important factor in landslide susceptibility mapping. Fig. 7 shows the spatial distribution of these factors, and it can be seen that the southern section cliffs present higher elevation because those areas are closer to the feet of the High Atlas Mountains.

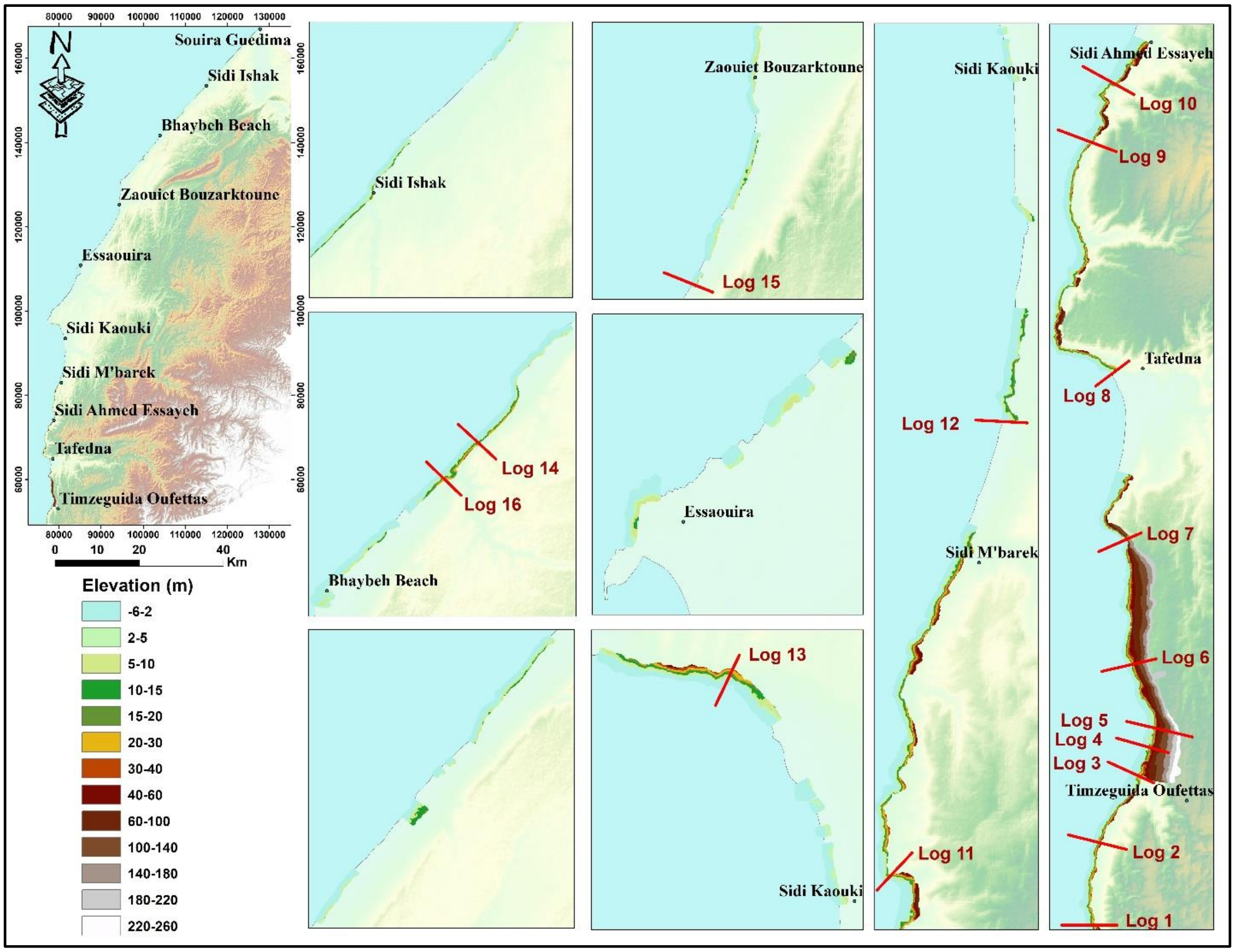

Fig. 7: The spatial distribution of elevation factor in the study area with profile emplacement

Other conditioning factors are provided by the fieldwork: i) the presence and type of cliff toe protection, as shown in Fig. 8 A, B, and C, either rock platform, slope deposit, or beach protection; ii) lithology tilting, which has a big impact on landslide occurrence, as shown in Fig. 8 D and E; iii) the presence of stream networks and springs in the cliff face which stimulate landslide occurrence; and iv) the presence of springs. Nine springs were localised, four of which are concentrated around Timzeguida Oufettas village which has a locally visible impact on landslide occurrence, particularly considering the presence of marls, which become more sliding when in contact with water. The other springs are in the southern section, except for one in the north between Bhaybeh beach and Sidi Ishak village. They considerably affect the mechanical processes that lead to slope failure and to the subsequent post-failure movements, particularly in the case of marls or clays.

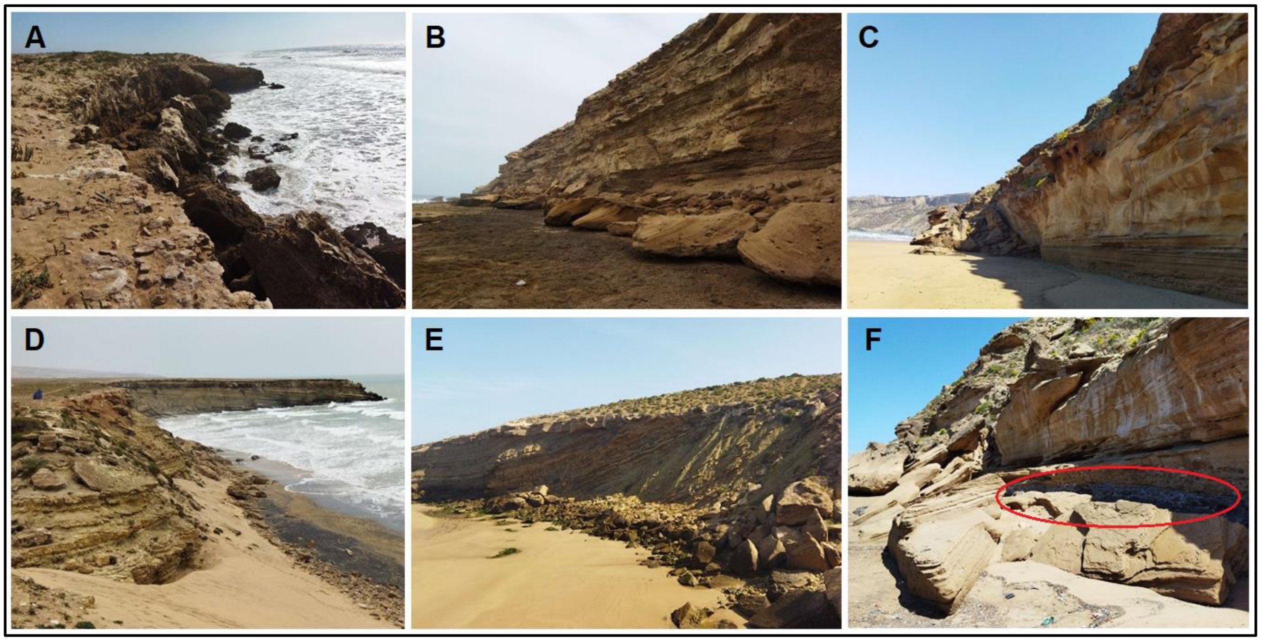

Fig. 8: Examples of some conditioning factors; A: absence of toe protection, B: rock platform protection, C: beach protection, D and E: tilted layers towards sea, and F: cliff toe lithology effect

For rainfall, the interpolation of rainfall records from four meteorological stations, from 1968 to 2015, was used to assess the spatial distribution of this conditioning factor. The results showed that the maximum average of 306 mm of precipitation fell around Essaouira city, while the precipitation values decreased towards the two extremities of the study area, reaching a minimum average precipitation of 252 mm.

Finally, the NDVI and land-use map were prepared from the Sentinel satellite image analysis, and six land-use types were extracted, including bare ground, cultivated areas, light vegetation, dense vegetation, roads and habitation, and breakwater areas.

4.3. Coastal landslide susceptibility assessment

Coastal landslide susceptibility using the IV method, as mentioned in the objectives, was produced considering two different susceptibility zonation approaches: susceptibility assessed at the pixel scale and considering ETUs.

4.3.1 By Pixel:

Table S1 presents the IV scores obtained for each class of each landslide conditioning factor used in the construction of each susceptibility model for 15 landslide inventory partitions defined according to their classification into shallow and deep-seated landslides, landslide type, or type of affected material (debris or rock).

The IV scores represent a clear contrast between the most and least favourable areas for the occurrence of different landslide types, and we describe the most important conditioning factors for each landslide type:

-For all landslide types (Model 1), the most relevant conditioning factor for the occurrence of all inventoried landslides are areas with slope angles > 45 (IV score = 1.377), followed by the solar radiation factor between 400 and 600 kWh/m2 (IV score = 1.332) and an elevation factor of 60–100 m (IV score = 1.320). The minimum value was obtained for the aspect class flat (IV score = -3.845). The results revealed, considering no landslide type or depth of the rupture surface differentiation, that slope angle and elevation are the most influent factors for landslide occurrence particularly in dry climate areas such as the Essaouira coastal cliff area, except for model 10 (rock topple), in which the slopes > 15º have negative scores.

Deep-seated landslides (Model 2), in the Essaouira coastal area, occurred more in areas with 400–600 kWh/m2 solar radiation (IV score = 1.536), in slope areas > 45° (IV score = 1.494), and in the high areas between 60 and 100 m (IV score = 1.480), where the minimum was in the same class as previous results. However, shallow mass movements occurred more in friable layers with an IV score of 3.011, in 600–700 kWh/m2 solar radiation (IV score = 2.072), and in areas with 35–45° slopes.

Rotational slides (Models 4, 5, and 6) generally occur in sandstone dolomites and dune sandstone with oblique stratification lithologies. For deep rotational slides, the grain size factor 38–51 (% sand) presented the highest value of 1.550, followed by slope angle factor class 30–40° with an IV score of 1.441. For shallow rotational slides, the grain size factor was strongly independent of the occurrence of this landslide type, with an IV score of 2.323.

-Translational slides (Models 7, 8, and 9), deep and shallow slides in the Essaouira coastal area, occur more in areas with 400–700 kWh/m2 solar radiation and in slope areas > 40°.

-Rock topple (Model 10). The grain size factor, particularly classes 0–11% silt (IV score = 2.092), 66–91% sand (IV score = 2.037), and 0–7% clay (IV score = 2.016), contribute more to the occurrence of rock topples, because they typically occur next to friable layers in the Essaouira coastal cliff area.

-Rock falls (Model 11) occur more in the “dune sandstone with oblique stratification” class of lithology factor, while the minimum IV value was -4.978 heterogeneous conglomerate, which is normal as rock falls do not occur in this lithology type.

-Rock slides (Model 12). The lumachelic clayey limestone lithology class presented a strong dependence on rock slides, with an IV score of 3.253, while the flat (-1) areas for the aspect factor presented a minimum IV score of -3.960.

-Debris fall and flow (Models 13 and 14). The lithological material with grain size sand 51–66% and silt 11–23% are more favourable to the occurrence of debris fall and debris flow in the Essaouira coastal area, and the slope angle factor class 0–2° is less favourable with an IV score of -4.822.

- Debris slides (Model 15) presented a strong dependence on the terrigenous red deposit class lithology factor, while the minimum was an IV score of -3.565 for the flat (-1) class aspect factor, which is normal because this landslide type occurs more in terrigenous lithologies and in slope areas.

To represent landslide susceptibility for each model, the final IV scores were reclassified into four classes: very low susceptibility (IV score < -1), low susceptibility (-1 < IV score < 0), moderate susceptibility (0 < IV score < 1), and high susceptibility (IV score > 1). Fig. 9 presents the spatial distribution of susceptibility classes for pixel-based landslide susceptibility Model 1. It can be observed that a very low susceptibility class appeared more in the northern section of the study area, whereas the southern section presented higher susceptibility to the occurrence of landslides, particularly because of the weight of the translational and rotational slides in those areas.

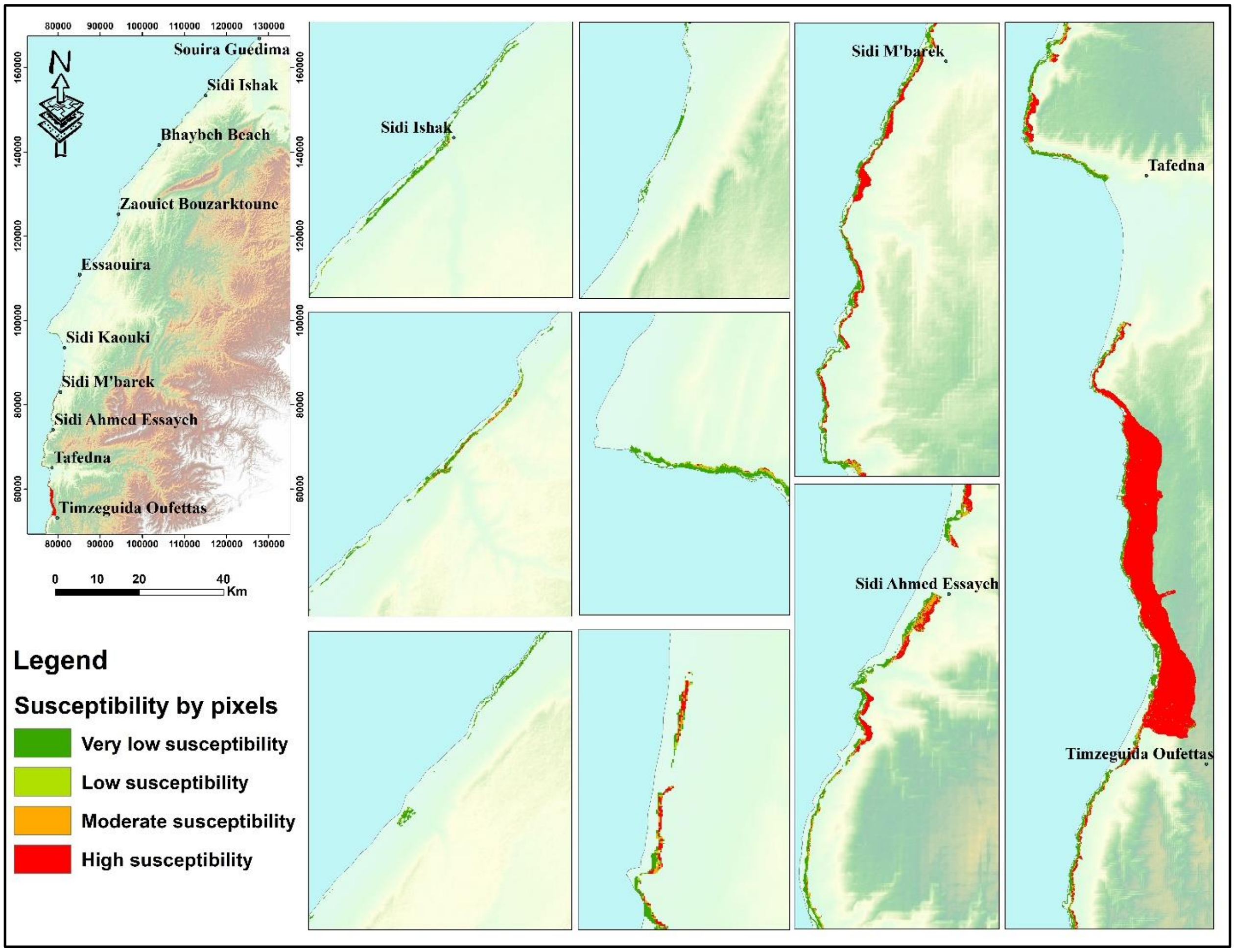

Fig. 9: Landslide susceptibility map using the pixel method

The IV model allowed for the classification of 38% of our study area with high susceptibility to the occurrence of all landslide types, while the very low susceptibility class was present in 56% of the study area (Table 5).

All other landslide type susceptibility models presented high percentages for the very low susceptibility class, with a maximum of 89.76% for debris slides. The exception is for debris flow, where the highest percentage was for high susceptibility with 53.85% of the study area.

Table 5: Percentage of landslide susceptibility classes

		Very low susceptibility	Low susceptibility	Moderate susceptibility	High susceptibility
Model 1	All landslides	55.45	2.55	2.66	39.35
Model 2	Deep-seated landslides	60.22	2.32	2.22	35.25
Model 3	Shallow landslides	72.58	4.10	3.80	19.52
Model 4	Rotational slides	52.71	7.02	6.55	33.72
Model 5	Deep rotational slides	55.03	5.84	5.95	33.18
Model 6	Shallow rotational slides	71.29	3.75	4.55	20.40
Model 7	Translational slides	61.08	2.42	2.07	34.43
Model 8	Deep translational slides	63.99	1.42	1.44	33.15
Model 9	Shallow translational slides	74.35	3.41	3.02	19.21
Model 10	Rock topple	67.41	5.52	5.95	21.12
Model 11	Rock fall	71.39	3.21	3.65	21.75
Model 12	Rock slides	80.02	2.72	2.56	14.70
Model 13	Debris fall	59.75	5.82	5.32	29.10
Model 14	Debris flow	39.15	3.04	3.96	53.85
Model 15	Debris slide	89.76	1.67	1.50	7.07

4.3.2 By ETUs

In general, the susceptibility assessment is conducted by classifying the ETUs into two classes: stabilised (37% of ETUs) and non-stabilised (63% of ETUs). The approach was performed individually for each type of landslide studied and shows that, for all landslide types, the unstable areas (classified as non-stabilised) are located more to the southern units of the study area.

To represent the ETU landslide susceptibility results, a zoomed section of the southern section of the study area next to Timzeguida Oufettas is presented (Fig. 10), for which landslide susceptibility zonation can be observed for the ETUs. This map presents the same allure or same variation as the susceptibility map produced by the pixel approach, except that, in the second ETU approach, ETU ID can be used to define the susceptible area in situ.

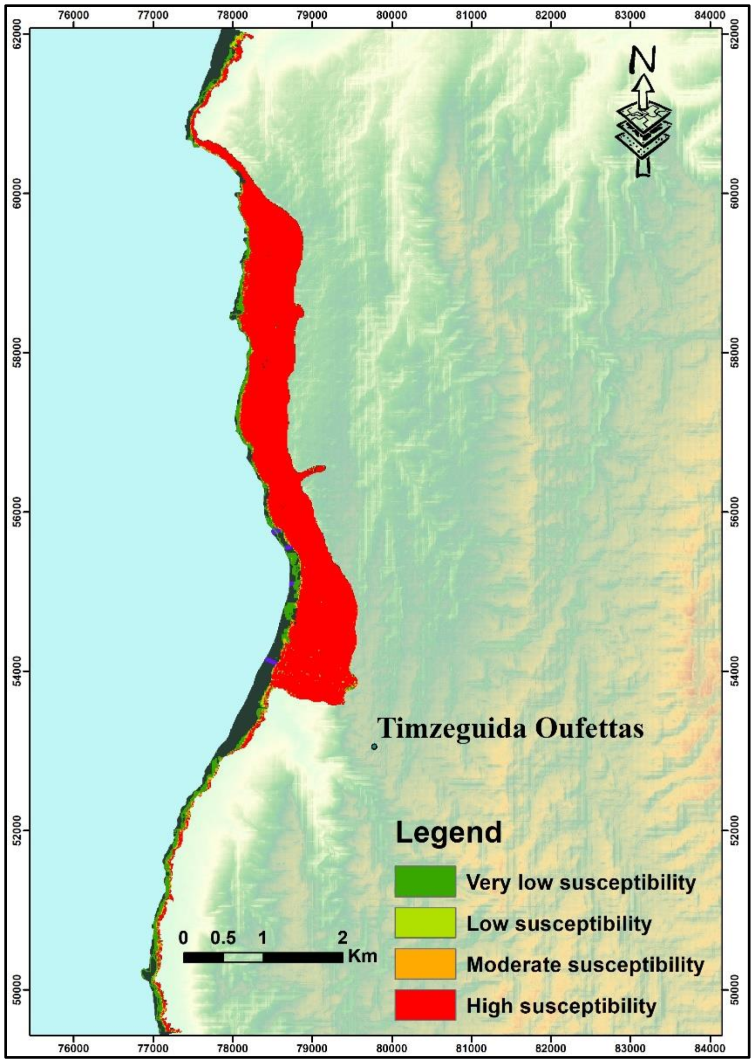

Fig. 10: Landslide susceptibility map using the ETU method for Model 1

4.4. Validation of coastal landslide susceptibility models

All coastal landslide susceptibility models were validated by spatial confrontation, with independent landslide partitions defined as validating subsets. ROC curves (Linden 2006; Remondo *et al.*, 2013) (Table 6) of the predictive models were computed, and the respective AUC values were calculated. Table 6 shows the AUC values obtained in the validation process for all models. We can remark that all landslide susceptibility models presented AUC values > 0.7, and Models 1, 4, 10, 13, and 14 (0.7 to 0.8) were considered acceptable. Models 2, 5, 6, 7, 8, and 9 (0.8 to 0.9) were considered excellent, and Models 3, 11, 12, and 15 (> 0.9) were considered outstanding.

Table 6: AUC values obtained in the validation process for all models

Models	Landslide type	AUC Low	AUC High	AUC values
Model 1	All landslides	0.751	0.842	0.798
Model 2	Deep-seated landslides	0.767	0.858	0.815
Model 3	Shallow landslides	0.735	1	0.92
Model 4	Rotational slides	0.694	0.872	0.794
Model 5	Deep rotational slides	0.709	0.889	0.813
Model 6	Shallow rotational slides	0.438	1	0.817
Model 7	Translational slides	0.759	0.854	0.809
Model 8	Deep translational slides	0.795	0.893	0.847
Model 9	Shallow translational slides	0.728	0.976	0.895
Model 10	Rock topple	0.25	1	0.75
Model 11	Rock fall	0.755	1	0.961
Model 12	Rock slides	0.827	1	0.948
Model 13	Debris fall	0.44	0.92	0.72
Model 14	Debris flow	0.561	0.878	0.731
Model 15	Debris slide	0.898	0.998	0.972

For total landslides (Model 1) with all factors, 0.710 (Fig. 11) was obtained. Next, the topographic wetness factor and rainfall factors were eliminated due to the dry climate of the area, and those factors did not present a strong dependence on the occurrence of landslides; a value of 0.798 (Fig. 11) was obtained, which means that the performance of Model 1 was improved in terms of prediction, particularly when low AUC values were obtained.

AUC graphs were plotted for translational slides (Model 7, 0.809; Fig. 12) and rotational slides (Model 4, 0.794; Fig. 13), as these two landslide types occupied approximately 85% of the unstable area in the pixel model approach. These results show that susceptibility models have good predictive skill and highlight the higher performance of predictive models when built for each type of landslide in comparison with the model built for the total landslides.

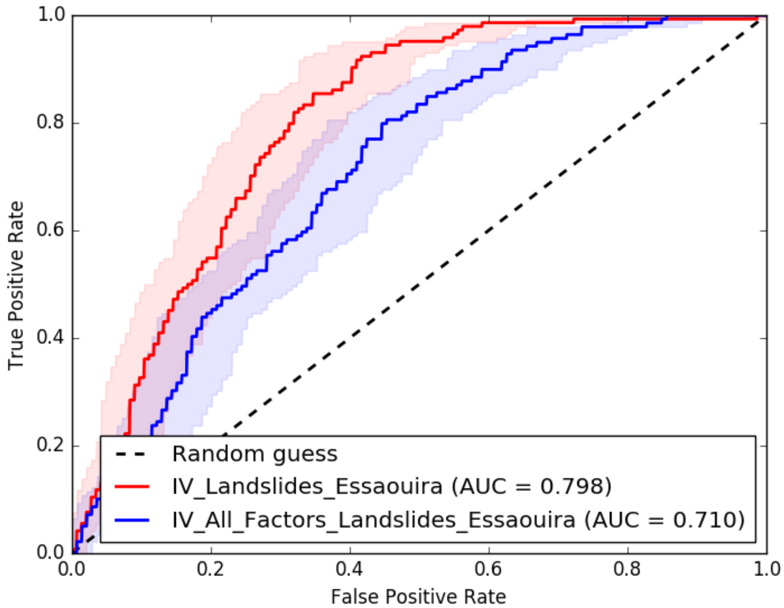

Fig. 11: ROC curves of the susceptibility model for all landslides with all factors (AUC = 0.710) and without TWI and rainfall factor (AUC = 0.798).

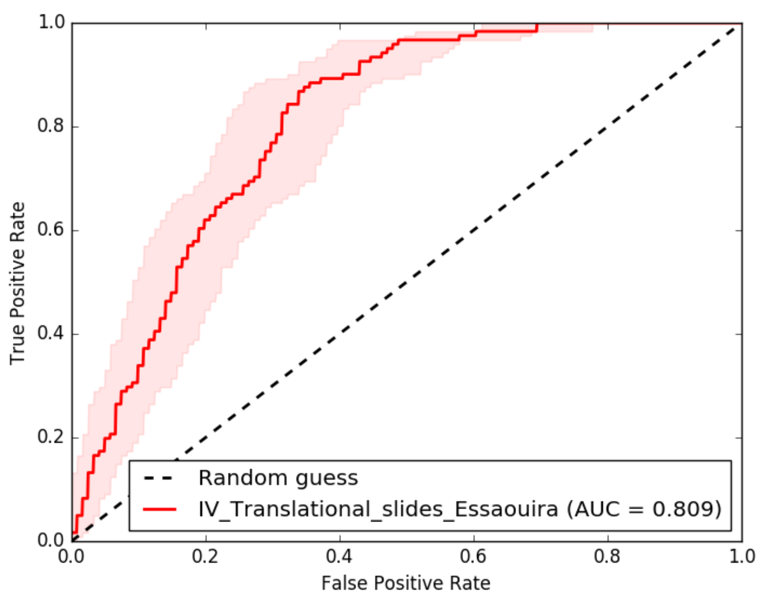

Fig. 12: ROC curves of the susceptibility model for translational slides (AUC = 0.809)

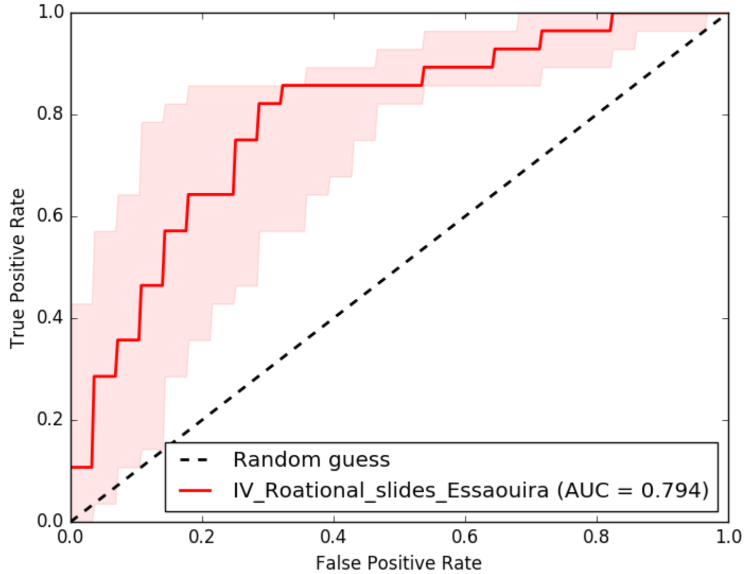

Fig. 13: ROC curves of the susceptibility model for rotational slides (AUC = 0.794)

5. Conclusion

The IV bivariate statistical approach to assess landslide susceptibility assessment in the 134 km of coastal area of Essaouira, based on geological and morphological analyses (interpretation of aerial photos, satellite images, and field survey), allowed for the classification of 38% of the study area with high susceptibility to landslide occurrence (using the pixel approach).

The translational slides followed by rotational slides occupied approximately 85% of the landslide area, which can be explained by the fact that the conditioning factors that contribute more to the occurrence of those landslides, namely > 45º slope angle, 400–700 kWh/m^2 solar radiation, and certain lithological formations, were all present in the study area, particularly the southern section. Another reason is that these landslide types typically occupy large areas.

Landslides are distributed along the entire study area, with a higher concentration in the southern section because of its topographic characteristics, mainly next to Sidi M'bark, Sidi Ahmed Essayeh, and in the northern sections of Tafedna and Timzguida Oufettas, while the less susceptible areas are located in the middle and northern sections of the Essaouira coastal area.

For all landslide types, the most important explanatory drivers are slope factor, particularly > 45°, solar radiation factor class 400–600 kWh/m2, and elevation class 60–100 m. These factors have already been highlighted by multiple authors as important conditioning factors of several landslide types. Most of the landslide susceptibility models (10 models out of 15) presented a strong interdependence with lithological factors or factors extracted from lithology, such as grain size and organic matter, which means that landslide occurrence is highly affected by lithological variations.

In the study area, precipitation was not present as a decisive conditioning factor, as a consequence of the spatial distribution of rainfall, since the highest values are concentrated around Essaouira City, which is more related to sandy coast subsystems.

To define in detail the spatial distribution of the most susceptible areas to the different landslide types along the Essaouira coastal area, particularly in the southern section next to Timzeguida Oufettas village, more in-depth studies are recommended.

Both the pixel and ETU models hold approximately the same value in all study areas. Based on these models, this study presents essential material for spatial planning and civil protection emergency actions in the Essaouira coastal area, particularly in the rocky coast subsystem.

Because ETUs are closer to the morphometry of the area, there is a more "guided" analysis in this approach compared with pixel-based analysis that is not related to a particular morphology on the cliff area. Both approaches have advantages and are inconvenient to use. The ETU approach considers cliff morphometry more and is more useful for territorial management interventions, however, it also leads to loss of susceptibility classification detail compared with the pixel approach, which is more relevant in terms of resolution.

6. References

Aleotti, P., Chowdhury, R.: Landslide hazard assessment: summary, review and new perspectives. Bull Eng Geol Environ 58:21–44, 1999.

Ammophiletea, Br.Bl., and Tüxen ex Westhoff, Dijk and Passchier: Coastal, Lagoon, Estuarian and Marine Ecosystems, 1946.

Andriani, G. F. , Walsh, N.: Rocky coast geomorphology and erosional processes: A case study along the Murgia coastline South of Bari, Apulia — SE Italy, https://doi.org/10.1016/j.geomorph.2006.03.033, Geomorphology journal, 2007

Bahir, M., Mennani, A., Jalal, M., Fakir, Y.: Impact de la sécheresse sur les potentialités hydriques de la nappe alimentant en eau potable la ville d'Essaouira (Mogador, Maroc). Sécheresse, 13(1): 13-9, 2002.

Bahir, M., Ouhamdouch, S., Carreira, P. M.: Water resource in Morocco face the climatic changes; study case of the Plio-Quaternary phreatic aquifer at the synclinal basin of Essaouira, Comunicações Geológicas (2016) 103, 1, 35-44, 2017

Balasubramani, K., Kumaraswamy, K.: Application of geospatial technology and information value technique in landslide Hazard zonation mapping: a case study of Giri Valley, Himachal Pradesh. Disaster Adv 6(1):38–47, 2013.

Beguería, S.: Validation and evaluation of predictive models in hazard assessment and risk management. Nat Hazards 37: 315-329, 2006.

Calvello, M., Cascini, L., Mastroianni, S.: Landslide zoning over large areas from a sample inventory by means of scale-dependent terrain units, Geomorphology journal. http://dx.doi.org/10.1016/j.geomorph.2012.10.026, 2015.

Chamchati, H., Bahir, M.: Potential Hydrogeological, Environment and Vulnerability to Pollution of the Plio-Quaternary Aquifers of the Coastal Basin of Essaouira (Morocco). Journal of Environment and Earth Science, 3(10): 170-185, 2013.

Chen, W., Sun, Z., Zhao, X., Lei, X., Shirzadi, A., & Shahabi, H.: Performance evaluation and comparison of bivariate statistical-based artificial intelligence algorithms for spatial prediction of landslides. ISPRS International Journal of Geo-Information, 9(12), 696, 2020.

Chimidi, G., Raghuvanshi, TK., Suryabhagavan, KV.: Landslide hazard evaluation and zonation in and around Gimbi town, western Ethiopia – a GIS-based statistical approach. Appl Geomat (Springer) 9(4):219–236, 2017.

Chkir, N., Trabelsi, R., Bahir, M., Hadj Ammar, F., Zouari, K., Chamchati, H., Monteiro, J. P.: Vulnérabilité des ressources en eaux des aquifères côtiers en zones semi-arides – Etude comparative entre les bassins d'Essaouira (Maroc) et de la Jeffara (Tunisie). Comunicações Geológicas, 95: 107-121, 2008.

Choubert, G., et Ambrogi, R.: Note préliminaire sur la présence de deux cycle sédimentaires dans le Pliocène marin au Maroc. N.M.S.G.M. t 7. n° 17. p. 3-72 Ont., 2, 4. 5), 1953.

Choubert, G., Faure-Muret, A., et Hotin ger, L.: La série stratigraphique de Tarfaya (Maroc sud-occidental) et le problème de la naissance de l'Océan Atlantique. N.M.S.G.M. 31, 237. p. 29-40 (lot.), 1971.

Cochet, A., et Combe, M.: Bassin d'Essaouira-Chichaoua et zone côtière d'Essaouira, Notes et Mémoires du Service Géologique n° 231, t. 2, p. 433-446, 1975.

Copernicus Sentinel data [14/05/2021]. Retrieved from ASF DAAC [11/11/2021], processed by ESA.

Corominas, J., Westen, C. Van, Frattini, P., Cascini, L., Malet, J.-P., Fotopoulou, S., Catani, F., Eeckhaut, M. Van Den, Mavrouli, O., Agliardi, F., Pitilakis, K., Winter, M. G., Pastor, M., Ferlisi, S., Tofani, V., Herva, J., and Smith, J. T.: Recommendations for the quantitative analysis of landslide risk, B. Eng. Geol. Environ., 73, 209–263, https://doi.org/10.1007/s10064-013-0538-8, 2014.

Dai, A. , and Lee, B.: Landslide characteristics and slope instability modeling using GIS, Lantau Island, Hong Kong, Geomorphology 42 (2002) 213 – 228, 2002.

Dikau, R., Brunsden, D., Schrott, L., Ibson, M.L.: Landslide Recognition: Identification, Movement and Causes. John Wiley & Sons, Chichester, UK, 1996.

Dufaud, F., Brun, L., et Planchut, B.: Le Basin du Sud-Ouest marocain, in Basin sédimentaires du Litoral africain. 1ère Partie, Littoral atlantique, Symposium de New-Delhi, 1964. de l'Asoc, des Services Géol. africains, p. 5-12 (Int., 1), 1966.

Earth Resources Observation and Science (EROS) Center, USGS EROS Archive - Aerial Photography - High Resolution Orthoimagery (HRO), 2018.

El mimouni, A., Daoudi, L.: Evolution à moyen terme du contexte hydrodynamique et morpho-sédimentaire la baie d'Essaouira (Maroc atlantique), XIIèmes Journées Nationales Génie Côtier – Génie Civil, 2012.

Elkadiri, R., Sultan, M., Youssef, A., Elbayoumi, T., Chase, R., Bulkhi, A., Al-Katheeri, M.: A remote sensing-based approach for debris-flow susceptibility assessment using artificial neural networks and logistic regression modeling. Selected topics in applied earth observations and remote sensing, IEEE J Sel Top Appl Earth Obs Remote Sens. doi:10.1109/JSTARS.2014.2337273, 2014.

Elmrabet, T., Levret, A., Ramdani, M., Tadili, B.: Historical seismicity in Morocco: Methodological aspects and cases of multidisciplinary evaluation, Commissariat à l'Energie Atomique, Institut de protection et de sureté nucléaire, Département d'Analyse de sureté, 1989.

Epifânio, B., Zêzere, J. L.,. Neves, M.: Susceptibility assessment to different types of landslides in the coastal cliffs of Lourinhã (Central Portugal), J. Sea Res. (2014), http://dx.doi.org/10.1016/j.seares.2014.04.006, 2014.

Epifânio, B., Zêzere, J.L., Neves, N.: Identification of hazardous zones combining cliff retreat with landslide susceptibility assessment. In: Conley, D.C., Masselink, G., Russel, P.E., O'Hare, T.J. (Eds.), Proceedings 12th International Coastal Symposium (Plymouth, England). Journal of Coastal Research, SI, 65, pp. 1681–1686, 2013.

Ercanoglu, M., Gokceoglu, C.: Use of fuzzy relations to produce landslide susceptibility map of a landslide prone area (West Black Sea Region, Turkey). Eng Geol 75:229–250. doi: 10.1016/j.enggeo.2004.06.001, 2004.

Fekri, A.: Contribution à l'étude hydrogéologique et hydrogéochimique de la zone synclinale d'Essaouira (bassin synclinal d'Essaouira). Thèse de doctorat, Université Cadi Ayyad, Maroc, 161, 1993.

Frattini, P., Crosta, G. & Carrara, A.: Techniques for evaluating the performance of landslide susceptibility models. Eng Geol 111: 62-72, 2010.

Gentile, W.: Caractérisation et suivi d'un champ dunaire par analyses sédimentologiques et télédétection (Essaouira-Cap Sim, Maroc Atlantique). Thèse Université de Province – Aix-Marseille I, 307 p, 1997.

Gilham, J. M.: Developing A Probabilistic Recession Model Through Characterisation and Quantification of the Erosion of Chalk Sea Cliffs in Brighton (Doctoral dissertation, University of Sussex), 2018.

Girma, F., Raghuvanshi, TK., Ayenew, T., Hailemariam, T.: Landslide hazard zonation in Ada Berga district, Central Ethiopia – a GIS based statistical approach. J Geom 9(i):25–38, 2015.

Gorsevski, PV., Gessler, PE., Foltz, RB., Elliot, WJ.: Spatial prediction of landslide hazard using logistic regression and ROC analysis. Trans GIS 10(3):395–415, 2006a.

Greenwood, R.O., Orford, J.D.: Factors controlling the retreat of Drumlin coastal cliffs in a low energy marine environment — Strangford Lough, Northern Ireland. J. Coast. Res. 23, 285–297, 2007.

Halam, A.: Mesozoic geology and the opening of the North-Atlantic. J. geol. 79, p. 129-157 (Int.), 1971.

Hampton, M. A., Griggs, G. B., Edil, T. B., Guy, D. E., Kelley, J. T., Komar, P. D., ... & Shipman, H. M.: Processes that govern the formation and evolution of coastal cliffs. US Geological Survey professional paper, 1693, 7-38, 2004.

Hamza, T. and Raghuvanshi, TK.: GIS based Landslide Hazard Evaluation and Zonation - A case from Jeldu District, Central Ethiopia. J King Saud Univ Sci 29(2):151–65, 2017.

Hander, M. : Contribution à l'étude de la bioclimatologie humaine au Maroc : l'exemple d'Essaouira, Thèse de Doctorat, Paris-IV, 356 p, 1993.

Heiri O., Lotter A. F. & Lemcke G.: Loss on ignition as a method for estimating organic and carbonate content in sediments: reproducibility and comparability of results. Journal of Paleolimnology, 25, 101–110, 2001.

Hungr, O., Leroueil, S., Picarelli, L.: The Varnes classification of landslide types, an update. Landslides 11 (2), 167–194, 2014.

Jade, S., Sarkar, S.: Statistical models for slope instability classification. Eng Geol 36(1–2):91–98, 1993.

Kanungo, DP., Arora, MK., Sarkar, S., Gupta, RP.: A comparative study of conventional, ANN black box, fuzzy and combined neural and fuzzy weighting procedures for landslide susceptibility zonation in Darjeeling Himalayas. Eng Geol 85:347–66, 2006.

Lan, HX., Zhou, CH., Wang, LJ., Zhang, HY., Li, RH.: Landslide hazard spatial analysis and prediction using GIS in the Xiaojiang watershed, Yunnan, China. Eng Geol 76:109–28, 2004.

Le Pichon, X.: La genèse de l'Atlantique Nord. La Recherche, n° 8. p. 21 (Int.), 1971.

Lee, S., Pradhan, B.: Landslide hazard mapping at selangor, malaysia using frequency ratio and logistic regression models. *Landslides*, *4*, 33–41, 2007.

Letortu, P., Costa, S., Maquaire, O., & Davidson, R.: Marine and subaerial controls of coastal chalk cliff erosion in Normandy (France) based on a 7-year laser scanner monitoring. Geomorphology, 335, 76-91, 2019.

Lharti, S., Flor, G., Daoudi, L., Flor, G.B., El mimouni A., Ben Ali, A.: Morfologia y Sedimentologia del complejo playa/dunas costeras de Essaouira (Marruecos atlantico) : modelo de transporte costero. Actas de la IX Reunión Nacional de Geomorfología, Santiago de Compostela (A. Pérez Alberti y J. López Bedoya, ed.), pp 401-417, 2006.

Lin, ML., Tung, CC.: A GIS-based potential analysis of the Landslides induced by the chi-chi earthquake. Eng Geol 71:63–77, 2003.

Linden, A.: Measuring diagnostic and predictive accuracy in disease management: an introduction to receiver operating characteristic (ROC) analysis. J Eval Clin Pract. 12: 132–139, 2006.

Mancini, F., Ceppi, C., Ritrovato, G.: GIS and statistical analysis for landslide susceptibility mapping in the Daunia area, Italy. Nat. Hazards Earth Syst. Sci. 10, 1851–1864, 2010.

Marques, F.: Sea cliff instability hazard prevention and planning: examples of practice in Portugal. J. Coast. Res. SI 56, 856–860, 2009.

Marques, F., Matildes, R., Redweik, P.: Statistically based sea cliff instability hazard assessment of Burgau-Lagos coastal section (Algarve, Portugal). Proceeding of the 11th International Coastal Symposium. Journal of Coastal Research, SI64: 927-931, 2011.

Marques, F.: Regional scale sea cliff hazard assessment at Sintra and Cascais counties, western coast of Portugal. Geosciences, 8(3), 80, 2018.

Marques, R.T.F.: Estudo de movimentos de vertente no concelho da Povoação (ilha de São Miguel, Açores): Inventariação, caracterização e análise da susceptibilidade. Ph.D. Thesis, Geological Risks, University of Azores, Ponta Delgada, Portugal, 2013.

Mateus, L. R., Frederico, G. S., & Cesar, F., Barella: Landslide susceptibility mapping using the statistical method of Information Value: A study case in Ribeirão dos Macacos basin, Minas Gerais, Brazil, Annals of the Brazilian Academy of Sciences, An Acad Bras Cienc (2021) 93(1): e20180897 DOI 10.1590/0001-3765202120180897, 2021.

Meena, S. R., Ghorbanzadeh, O. and Blaschke, T.: A Comparative Study of Statistics-Based Landslide Susceptibility Models: A Case Study of the Region Affected by the Gorkha Earthquake in Nepal, *ISPRS Int. J. Geo-Inf.*, https://doi.org/10.3390/ijgi8020094, 2019.

Mengistu, F., Suryabhagavan, KV., Raghuvanshi, TK., Lewi, E.: Landslide Hazard zonation and slope instability assessment using optical and InSAR data: a case study from Gidole town and its surrounding areas, southern Ethiopia. Remote Sensing of Land 3(1):1–14, 2019.

Mennani, A.: Apports de l'hydrochimie et de l'isotopie à la connaissance du fonctionnement des aquifères de la zone côtière d'Essaouira. Thèse de doctorat, Université Cadi Ayyad, Maroc, 152, 2001.

Michard, A., Westphal, M., Bosert, A., et Hamzeh, R.: Tectonique de blocs dans le socle atlaso-mésétien du Maroc : une nouvelle interprétation des données géologiques et paléomagnétiques. Earth Plan. Sci. Let. 24, p. 363-68 (Int.), I975.

Moore, L.J., Griggs, G.B.: Long-term cliff retreat and erosion hotspots along the central shores of the monterey bay national marine sanctuary. Mar. Geol. 181 (1–3), 265–283, 2002.

Moore, R., & Davis, G.: Cliff instability and erosion management in England and Wales. Journal of Coastal Conservation, 19(6), 771-784, 2015.

Neves, M., Ramos-Pereira, A.: The interaction between marine and sub-aerial processes in the evolution of rocky coasts: the example of Castelejo (southwest Portugal). Bol. Inst. Esp. Oceanogr. 15, 251–258, 1999.

Neves, M., Zêzere, J.L., Henriques, C.: Garcia, R., Oliveira, S., Piedade, A., Modeling the long term evolution of rocky coasts in central Portugal. Avances de la Geomorfología en España. Actas de la XII Reunión Nacional de Geomorfología pp. 73–76, 2012.

Oliveira, S. C., Catalão, J., Ferreira, Ó., Alveirinho D. J.: Evaluation of cliff retreat and beach nourishment in southern Portugal using photogrammetric techniques. Journal of Coastal Research, 24(4A): 184-193. https://doi.org/10.2112/06-0781.1, 2008

Oliveira, S. C., Zêzere, J.L., Lajas, S., Melo, R.: Combination of statistical and physically based methods to assess shallow slide susceptibility at the basin scale. Natural Hazards and Earth System Science, 17, 1091–1109, https://doi.org/10.5194/nhess-17-1091-2017, 2017

Pawluszek, K.: Landslide features identifcation and morphology investigation using high-resolution DEM derivatives, Natural Hazards (2019) 96:311–330 https://doi.org/10.1007/s11069-018-3543-1, 2019

Pereira, S., Santos, P.P., Zêzere, J.L., Tavares, A.O., Garcia, R.A.C., Oliveira, S.C.: A landslide risk index for municipal land use planning in Portugal. *Science of the Total Environment*, 735: 139463. https://doi.org/10.1016/j.scitotenv.2020.139463, 2020

Petley, DN.: The global occurrence of fatal landslides in 2007. Geophysical Research Abstracts, vol. 10, EGU General Assembly 2008, p 3, 2008.

Queiroz, S. M., & Marques, F. M.: Sea cliff instability susceptibility considering nearby human occupation and predictive capacity assessment. Engineering Geology, 253, 75-93, 2019.

Reichenbach, P., Rossi, M., Malamud, B. D., Mihir, M. and Guzzetti, F.: A review of statistically-based landslide susceptibility models, https://doi.org/10.1016/j.earscirev.2018.03.001, *2018.*

Remondo, J., González, A., Díaz De Terán, J. R., Cendrero, A., Fabbri A., and Chung, C. J. F.: Validation of Landslide Susceptibility Maps; Examples and Applications from a Case Study in Northern Spain, Natural Hazards 30: 437–449, 2003.

Rocha, J., Ferreira, J. C., Simões, J., & Tenedório, J. A.: Modelling coastal and land use evolution patterns through neural network and cellular automata integration. Journal of Coastal Research, SPEC. ISSUE 50, 827–831, 2007

Saadi, M.: Relations des alignements structuraux au Maroc avec différents phénomènes géologiques et leur contribution à la compréhension de l'évolution structurale du pays. N.M.S.G.M., 236, p. 13-18 (Int.), 1972.

Shahabi, H., Khezri, S., Ahmad, B.B., Hashim, M.: Landslide susceptibility mapping at Central Zab Basin, Iran: A comparison BETWEEN analytical hierarchy process, frequency ratio and logistic regression models. *Catena*, *115*, 55–70, 2014.

Shano, L., Raghuvanshi, T. K. and Meten, M.: Landslide susceptibility evaluation and hazard zonation techniques – a review, geoenvironmental-disasters, springer open, 2020.

Simon, C.: Le géo-système dunaire anthropisé d'Essaouira – est (Maroc Atlantique) dynamique et paléo-environnements. Thèse de doctorat. Univ. Aix Marseille I, 204 p, 2000.

Smaij, Z.: Typologie de la qualité des ressources en eaux du bassin de Tensift Al-Haouz et cadre juridique de protection et de préservation. Université Cadi Ayyad Faculté des sciences et techniques. Marrakech. 96p, 2011.

Sunamura, T.: Geomorphology of rocky coasts. Wiley, Chichester. 302 pp, 1992.

Sunamura, T.: Rocky coast processes: with special reference to the recession of soft rock cliffs doi: 10.2183/pjab.91.481 ©2015 The Japan Academy, 2015

Taleb, M.S., Fennane, M.: Vascular Plant Communities of Morocco, Geobotany Studies, Springer International Publishing AG, part of Springer Nature, 2019.

Teixeira M.: Movimentos de Vertente: Factores de Ocorrência e Metodologia de Inventariação. Geonovas (20):12 p, 2006.

Teixeira, M., Bateira, C., Marques, F., & Vieira, B.: Physically based shallow translational landslide susceptibility analysis in Tibo catchment, NW of Portugal. Landslides, 12(3), 455-468, 2015.

Trenhaile, AS.: The Geomorphology of Rock Coasts. Oxford: Oxford University Press, 384p, 1987.

Van Den Eeckhaut, M., Reichenbach, P., Guzzetti, F., Rossi, M., Poesen, J.: Combined landslide inventory and susceptibility assessment based on different mapping units: an example from the Flemish Ardennes, Belgium. Nat. Hazards Earth Syst. Sci. 9, 507–521, 2009.

Van Westen, C.J., van Asch, T.W.J., Soeters, R.: Landslide hazard and risk zonation — why is it still so difficult? Bull. Eng. Geol. Environ. 65, 167–184, 2006.

Van Westen, CJ., Castellanos, E., Kuriakose, SL.: Spatial data for landslide susceptibility, hazard, and vulnerability assessment: an overview. Eng Geol 102:112–131, 2008.

Van Westen, CJ., Rengers, N., Terlien, MTJ., Soeters R.: Prediction of the occurrence of slope instability phenomenal through GIS-based hazard zonation. Geol Rundsch 86(2):404–14, 1997.

Varnes, D.J.: International Association of Engineering Geology Commission on Landslides and Other Mass Movements on Slopes. Landslide Hazard Zonation: A Review of Principles and Practice UNESCO, Paris, 1984.

Varnes, D.J.: Slope movement types and processes. In: Schuster, R.L., Krizek, R.J. (Eds.), Special Report 176: Landslides: Analysis and Control. Transportation and Road Research Board, National Academy of Science, Washington D. C., pp. 11–33, 1978.

Varnes, DJ.: Landslide types and processes. In: Turner AK, Schuster RL (eds) Landslides: investigation and mitigation, Transportation Research Board special report 247. National Academy Press, National Research Council, Washington, D.C, 1996.

Violante, C.:Rocky coast: geological constraints for hazard assessment,Geological Society, London, Special Publications, 322, 1-31, 1 January 2009, https://doi.org/10.1144/SP322.1, 2009

Wang, L.-J., Guo, M., Sawada, K., Lin, J., Zhang, J.: A comparative study of landslide susceptibility maps using logistic regression, frequency ratio, decision tree, weights of evidence and artificial neural network. *Geosci. J.*, *20*, 117–136, 2016.

Weisrock, A.: Géomorphologie et paléo-environnements de l'Atlas atlantique (Maroc). Thèse d'état, Paris I, 931 p, 1980.

WP/WLI.: International Geotechnical Societies' UNESCO (Working Party on World Landslide Inventory), Multilingual Landslide Glossary. Bitech Publisher, Richmond, British Columbia, Canada, 1993.

Yalcin, A.: GIS-based landslide susceptibility mapping using analytical hierarchy process and bivariate statistics in Ardesen (Turkey): comparisons of results and confirmations. Catena 72:1–12, 2008.

Yin, K.L., Yan, T.Z.: Statistical prediction models for slope instability of metamorphosed rocks. In: Bonnard, C. (Ed.), Proceedings of the 5th International Symposium on Landslides (Lausanne, Switzerland), 2, pp. 1269−1272, 1988.

Zêzere, J. L., Reis, E., Garcia, R., Oliveira, S., Rodrigues, M. L., Vieira, G., and Ferreira, A. B.: Integration of spatial and temporal data for the definition of different landslide hazard scenarios in the area north of Lisbon (Portugal), Nat. Hazards Earth Syst. Sci., 4, 133–146, https://doi.org/10.5194/nhess-4-133-2004, 2004.

Zêzere, J.L.: Landslide susceptibility assessment considering landslide typology. A case study in the area north of Lisbon (Portugal). Nat. Hazards Earth Syst. Sci. 2, 73–82, 2002.

Zêzere, J.L.: Pereira, S., Melo, R., Oliveira, S.C., Garcia, R.A.C., Mapping landslide susceptibility using data-driven methods. Science of the Total Environment 589, 250–267, 2017.